

This discussion paper is/has been under review for the journal Atmospheric Chemistry and Physics (ACP). Please refer to the corresponding final paper in ACP if available.

# Iodine's impact on tropospheric oxidants: a global model study in GEOS-Chem

T. Sherwen<sup>1</sup>, M. J. Evans<sup>1,2</sup>, L. J. Carpenter<sup>1</sup>, S. J. Andrews<sup>1</sup>, R. T. Lidster<sup>1</sup>,  
B. Dix<sup>3</sup>, T. K. Koenig<sup>3,4</sup>, R. Volkamer<sup>3,4</sup>, A. Saiz-Lopez<sup>5</sup>, C. Prados-Roman<sup>5</sup>,  
A. S. Mahajan<sup>6</sup>, and C. Ordóñez<sup>7</sup>

<sup>1</sup>Wolfson Atmospheric Chemistry Laboratories (WACL), Department of Chemistry,  
University of York, York, YO10 5DD, UK

<sup>2</sup>National Centre for Atmospheric Science (NCAS), University of York, York, YO10 5DD, UK

<sup>3</sup>Department of Chemistry and Biochemistry, University of Colorado, Boulder,  
CO 80309-0215, USA

<sup>4</sup>Cooperative Institute for Research in Environmental Sciences, University of Colorado,  
Boulder, CO 80309-021, USA

<sup>5</sup>Atmospheric Chemistry and Climate Group, Institute of Physical Chemistry Rocasolano,  
CSIC, Madrid, 28006, Spain

<sup>6</sup>Indian Institute of Tropical Meteorology, Maharashtra, 411008, India

<sup>7</sup>Met Office, FitzRoy Road, Exeter, EX1 3PB, UK

ACPD

15, 20957–21023, 2015

Iodine's impact on  
tropospheric  
oxidants: a global  
model study in  
GEOS-Chem

T. Sherwen et al.

Title Page

Abstract

Introduction

Conclusions

References

Tables

Figures

◀

▶

Back

Close

Full Screen / Esc

Printer-friendly Version

Interactive Discussion



Received: 29 June 2015 – Accepted: 13 July 2015 – Published: 5 August 2015

Correspondence to: T. Sherwen (ts551@york.ac.uk)

Published by Copernicus Publications on behalf of the European Geosciences Union.

ACPD

15, 20957–21023, 2015

---

Iodine's impact on  
tropospheric  
oxidants: a global  
model study in  
GEOS-Chem

T. Sherwen et al.

---

[Title Page](#)

[Abstract](#)

[Introduction](#)

[Conclusions](#)

[References](#)

[Tables](#)

[Figures](#)

◀

▶

[Back](#)

[Close](#)

[Full Screen / Esc](#)

[Printer-friendly Version](#)

[Interactive Discussion](#)

## Abstract

We present a global simulation of tropospheric iodine chemistry within the GEOS-Chem chemical transport model. This includes organic and inorganic iodine sources, standard gas-phase iodine chemistry and simplified higher iodine oxide ( $I_2O_X$ ,  $X = 2, 3, 4$ ) chemistry, photolysis, deposition and parametrised heterogeneous reactions. In comparisons with recent Iodine Oxide (IO) observations the iodine simulation shows an average bias of  $\sim +66\%$  available surface observations in the marine boundary layer (outside of polar regions), and of  $\sim +73\%$  within the free troposphere ( $350 < hPa < 900$ ) over the eastern Pacific. Iodine emissions ( $3.8 \text{ Tg yr}^{-1}$ ) are overwhelmingly dominated by the inorganic ocean source, with 76 % of this emission from Hypoiodous acid (HOI). HOI is also found to be the dominant iodine species in terms of global tropospheric  $I_Y$  burden (contributing up to 70 %). The iodine chemistry leads to a significant global tropospheric  $O_3$  burden decrease (9.0 %) compared to standard GEOS-Chem (v9-2). The iodine-driven  $O_X$  loss rate ( $748 \text{ Tg O}_X \text{ yr}^{-1}$ ) is by photolysis of HOI (78 %), photolysis of OIO (21 %), and reaction of IO and BrO (1 %). Increases in global mean OH concentrations (1.8 %) by increased conversion of hydroperoxy radicals exceeds the decrease in OH primary production from the reduced  $O_3$  concentration. We perform sensitivity studies on a range parameters and conclude that the simulation is sensitive to choices in parameterisation of heterogeneous uptake, ocean surface iodide, and  $I_2O_X$  ( $X = 2, 3, 4$ ) photolysis. The new iodine chemistry combines with previously implemented bromine chemistry to yield a total bromine and iodine driven tropospheric  $O_3$  burden decrease of 14.4 % compared to a simulation without iodine and bromine chemistry in the model. This is a significant impact and so halogen chemistry needs to be considered in climate and air quality models.

ACPD

15, 20957–21023, 2015

Iodine's impact on  
tropospheric  
oxidants: a global  
model study in  
GEOS-Chem

T. Sherwen et al.

|  |                              |
|--|------------------------------|
| <a href="#">Title Page</a>               |                              |
| <a href="#">Abstract</a>                 | <a href="#">Introduction</a> |
| <a href="#">Conclusions</a>              | <a href="#">References</a>   |
| <a href="#">Tables</a>                   | <a href="#">Figures</a>      |
| <a href="#">◀</a>                        | <a href="#">▶</a>            |
| <a href="#">◀</a>                        | <a href="#">▶</a>            |
| <a href="#">Back</a>                     | <a href="#">Close</a>        |
| <a href="#">Full Screen / Esc</a>        |                              |
| <a href="#">Printer-friendly Version</a> |                              |
| <a href="#">Interactive Discussion</a>   |                              |

# 1 Introduction

The chemistry of the troposphere controls the concentration of a range of climate gases including ozone ( $O_3$ ) and methane ( $CH_4$ ) (Kim et al., 2011; Voulgarakis et al., 2013; Young et al., 2013), and determines human and agriculture exposure to air quality

5 pollutants such as  $O_3$  and aerosols (Ainsworth et al., 2012; Fiore et al., 2012; Fowler et al., 2008). The chemical cycles maintaining concentrations of these atmospheric constituents are complex, and depend strongly upon the concentrations of  $O_3$  and of the hydroxyl radical ( $OH$ ) as key oxidants. Understanding the budgets and controls on these gases is therefore central to assessments of tropospheric chemistry (Voulgarakis et al., 2013).

10 The chemistry of  $O_3$  and  $OH$  in the troposphere is coupled and the central aspects of this are well known (Young et al., 2013). The photolysis of  $O_3$  produces an electronically excited oxygen atom ( $O(^1D)$ ), which can react with a water molecule to produce two  $OH$  radicals. Subsequent reaction of  $OH$  with organic compounds (hydrocarbons, 15 oxygenates, methane, carbon monoxide etc.) produces peroxy radicals ( $RO_2$ ). If sufficient nitrogen oxide ( $NO$ ) is available, the dominate fate of  $RO_2$  radicals is to oxidise  $NO$  to nitrogen dioxide ( $NO_2$ ), allowing the formation of  $O_3$  via photolysis of  $NO_2$  (Atkinson, 2000). Tropospheric  $O_3$  also has a source via transport from the stratosphere, and is lost to the Earth's surface via dry deposition.

20 Over the last decades significant research effort has gone into understanding the production of  $O_3$ , typically over continental regions due to its adverse impact on health and food security (Ainsworth et al., 2012; Fowler et al., 2008). However less emphasis has been placed on its loss through chemical destruction.  $O_3$  is chemically lost in the troposphere predominantly through its photolysis in the presence of water to produce  $OH$ . Secondary sinks include reaction with  $HO_2$  or  $OH$  (Lelieveld and Dentener, 2000). 25 Bromine and iodine compounds have also been identified as additional sinks for  $O_3$  and as perturbations to  $OH$  cycling (Chameides and Davis, 1980; von Glasow et al., 2004). Of the two compounds iodine has arguably the more complex chemistry due to

[Title Page](#)[Abstract](#)[Introduction](#)[Conclusions](#)[References](#)[Tables](#)[Figures](#)[|◀](#)[▶|](#)[◀](#)[▶](#)[Back](#)[Close](#)[Full Screen / Esc](#)[Printer-friendly Version](#)[Interactive Discussion](#)

its many oxidation states, ability to form higher iodine oxides ( $I_2O_X$ ,  $X \geq 2$ ) and iodine particles (Saiz-Lopez et al., 2012b). There are significant uncertainties in iodine chemistry kinetics, and a rapidly evolving body of knowledge on iodine sources which we now describe.

Historically the dominant source of iodine in the atmosphere was thought to be iodinated organic compounds from the ocean. Initially methyl iodide ( $CH_3I$ ) was considered the largest source but it was realised that even at the low observed concentration the very fast photolysis rates of other organo-halogens would lead to them playing a significant role (Chuck et al., 2005; Jones et al., 2010; Law and Sturges, 2006). More recently, emission of inorganic halogen compounds ( $I_2$  and HOI) has been identified as a potentially significant flux of iodine into the atmosphere (Carpenter et al., 2013). This mechanism was originally proposed by Garland and Curtis (1981) whereby  $O_3$  uptake to the ocean and the subsequent reaction with Iodide ( $I^-$ ) leads to volatilisation of inorganic iodine from the ocean. Based on laboratory studies, fluxes of HOI and  $I_2$  have been parameterised as a function of surface iodide concentration,  $O_3$  concentration, 10 m wind speed and surface temperature (Carpenter et al., 2013; MacDonald et al., 2014).

Our understanding of the chemistry of iodine has been described in detail in recent publications (Saiz-Lopez et al., 2012b; Sommariva et al., 2012). Once emitted into the atmosphere, the highly labile iodinated precursors rapidly photolysis with lifetimes of seconds (e.g.  $I_2/HOI$ ) to days (e.g.  $CH_3I$ ) to release atomic iodine. The iodine can catalytically destroy  $O_3$  by the reaction with of  $O_3 + I$  to form IO, followed by secondary reactions ( $+HO_2$ ,  $+IO$ ,  $+NO_2$ ,  $+BrO$ ) which can regenerate atomic I without the abstracted oxygen. For instance IO reacts with  $HO_2$ , leading to HOI formation, and this is rapidly photolysed to reform I causing a net conversion of  $HO_2$  to OH (Reaction R11).

A large body of experimental and theoretical work has been evaluated in JPL/IUPAC compilations (Atkinson et al., 2007, 2000; Sander et al., 2011). Whilst the key iodine reactions for processes of interest such as  $O_3$  destruction (e.g. HOI, OIO photolysis) are now relatively well defined, the experimental rate data are limited or non-existent for

Iodine's impact on tropospheric oxidants: a global model study in GEOS-Chem

T. Sherwen et al.

[Title Page](#)

[Abstract](#)

[Introduction](#)

[Conclusions](#)

[References](#)

[Tables](#)

[Figures](#)

[|◀](#)

[▶|](#)

[◀](#)

[▶](#)

[Back](#)

[Close](#)

[Full Screen / Esc](#)

[Printer-friendly Version](#)

[Interactive Discussion](#)



certain processes. For example,  $I_2O_X$  ( $X \geq 2$ ) photolysis cross-sections and quantum yields, heterogeneous uptake parameters and the ultimate chemical fate are all poorly quantified, yet these reactions can significantly affect the  $IO_X$  lifetime.  $I_2O_X$  ( $X \geq 2$ ) forms through combination reactions (R1)–(R5) however questions remain about their polymerisation, photolytic properties and eventual fate as discussed further by Saiz-Lopez et al. (2012b). Recent work has shown some of the key iodine species to be well buffered to mechanism uncertainties, but highlights the sensitivity of iodine concentrations and hence atmospheric impacts of this higher oxide chemistry (Sommariva et al., 2012).



15 Due to their short lifetimes and low atmospheric concentrations measuring iodine species poses significant challenges and so the observational dataset is sparse. For decades, measurements have focused on organic compounds and mainly  $CH_3I$  (Saiz-Lopez et al., 2012b). Technique development for in-situ measurements has led to an increase in data availability over the last decade, for both organic (e.g.  $CH_3I$  and  $CH_2IX$ , with  $X = Cl, Br, I$ ) and inorganic (e.g.  $IO$ ,  $OIO$ ,  $I_2$ ) species (Saiz-Lopez et al., 2012b). Satellites may offer a mechanism to obtain global coverage, but retrievals at the low tropospheric concentrations are problematic (Schonhardt et al., 2008).

20 Recent organic and inorganic measurements from aircraft (Dix et al., 2013; Volkamer et al., 2015; Wang et al., 2015), balloons (Butz et al., 2009), mountain tops (Puente-dura et al., 2012), ground stations (Lawler et al., 2014; Mahajan et al., 2010; Read et al., 2008) and cruises (Großmann et al., 2013; Jones et al., 2010; Mahajan et al., 2012) are establishing the global ubiquity of iodine compounds over the oceans. This increase in observations has enabled the development of global organic halogen emis-

|  |                              |
|--|------------------------------|
| <a href="#">Title Page</a>               |                              |
| <a href="#">Abstract</a>                 | <a href="#">Introduction</a> |
| <a href="#">Conclusions</a>              | <a href="#">References</a>   |
| <a href="#">Tables</a>                   | <a href="#">Figures</a>      |
| <a href="#">◀</a>                        | <a href="#">▶</a>            |
| <a href="#">◀</a>                        | <a href="#">▶</a>            |
| <a href="#">Back</a>                     | <a href="#">Close</a>        |
| <a href="#">Full Screen / Esc</a>        |                              |
| <a href="#">Printer-friendly Version</a> |                              |
| <a href="#">Interactive Discussion</a>   |                              |

sions (Ordóñez et al., 2012) and more recently, datasets of IO observations with extensive geographical coverage (Prados-Roman et al., 2015b; Volkamer et al., 2015; Wang et al., 2015).

Although the increase in coverage and type of observations has somewhat improved constraints of iodine compounds, the recently suggested inorganic ocean source ( $\text{HOI}/\text{I}_2$ ) required to reproduce observed concentrations of IO (Großmann et al., 2013; Gómez Martín et al., 2013; Jones et al., 2010; Mahajan et al., 2010) remains unconstrained by in-situ direct flux observations. However, observations of marine boundary layer  $\text{I}_2$  concentrations have been made recently (Lawler et al., 2014). The inorganic iodide emission requires knowledge of surface seawater iodide concentrations, but global iodide data remain spatially limited (Chance et al., 2014), and further complexities such as suppression of iodine emissions by dissolved organic matter also add uncertainty to the flux (Shaw and Carpenter, 2013).

Iodine chemistry has been evaluated by a number of box model studies (Sander et al., 1997; Mahajan et al., 2009; McFiggans et al., 2000, 2010; Read et al., 2008; Saiz-Lopez et al., 2007) and a few global model studies (Prados-Roman et al., 2015a; Saiz-Lopez et al., 2012a, 2014). The initial focus was predominantly on geographic regions with elevated concentrations (e.g. polar Sander et al., 1997; Saiz-Lopez et al., 2007 and coastal Mahajan et al., 2009; McFiggans et al., 2000; Saiz-Lopez et al., 2006) and attempted to explain localised chemical perturbations mainly through the use of box models. Iodine-driven  $\text{O}_3$  loss was found to proceed through IO self reaction (Reactions R6–R8) at high IO concentrations ( $> 2 \text{ pptv}$ ),



## Iodine's impact on tropospheric oxidants: a global model study in GEOS-Chem

T. Sherwen et al.

[Title Page](#)

[Abstract](#)

[Introduction](#)

[Conclusions](#)

[References](#)

[Tables](#)

[Figures](#)

[|◀](#)

[▶|](#)

[◀](#)

[▶](#)

[Back](#)

[Close](#)

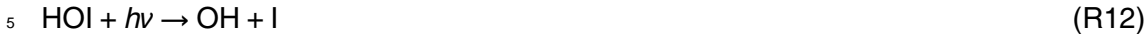
[Full Screen / Esc](#)

[Printer-friendly Version](#)

[Interactive Discussion](#)



through  $\text{HO}_2$  (Reactions R10–R12) at lower IO concentrations (Saiz-Lopez et al., 2012b),



and by reactions between IO and BrO (Reactions R14–R17) where BrO concentrations are high.



When considered alongside bromine chemistry, box model studies have shown the magnitude of these halogen driven  $\text{O}_3$  loss processes to be up to 45 % (Mahajan et al., 2009; Read et al., 2008) of the total loss. Iodine can change the local  $\text{HO}_2 : \text{OH}$  ratio due to the production of HOI from  $\text{HO}_2$  and IO (Reaction R11), and its subsequent photolysis to release OH (Reaction R12) (Bloss, 2005; Chameides and Davis, 1980). Perturbation to the  $\text{NO} : \text{NO}_2$  ratio has been shown to be significant at higher IO concentrations in polluted coastal locations (McFiggans et al., 2010) due to the ability of IO to oxidize NO into  $\text{NO}_2$ , which affects  $\text{O}_3$  production. More recently, measurements in the marine boundary layer on ground-based island monitoring stations (Read et al., 2008; Mahajan et al., 2010; Gómez Martín et al., 2013), on ships (Großmann et al., 2013; Mahajan et al., 2010; Prados-Roman et al., 2015b), by balloon (Butz et al., 2009), and by aircraft (Dix et al., 2013; Volkamer et al., 2015; Wang et al., 2015) have demon-

Title Page

Abstract

Introduction

Conclusions

References

Tables

Figures

|◀

▶|

Back

Close

Full Screen / Esc

Printer-friendly Version

Interactive Discussion

**Iodine's impact on tropospheric oxidants: a global model study in GEOS-Chem**

T. Sherwen et al.

[Title Page](#)[Abstract](#)[Introduction](#)[Conclusions](#)[References](#)[Tables](#)[Figures](#)[|◀](#)[▶|](#)[◀](#)[▶](#)[Back](#)[Close](#)[Full Screen / Esc](#)[Printer-friendly Version](#)[Interactive Discussion](#)

strated that these O<sub>3</sub> loss processes also occur in remote locations (e.g. non-coastal). These studies highlight the vertical and global extent of iodine chemistry.

Recently, the role of reactive halogens have also been investigated in global chemical transport models (Parrella et al., 2012) and chemistry-climate models (Ordóñez et al., 2012; Saiz-Lopez et al., 2014). A study considering only bromine chemistry reported significant impacts on OH concentrations and O<sub>3</sub> burdens with decreases of 4 and 6.5 %, respectively (Parrella et al., 2012). In a different study with a different model, inclusion of tropospheric bromine, iodine and chlorine chemistry led to topical tropospheric marine average O<sub>3</sub> columns to decrease on the order of 10 % (Saiz-Lopez et al., 2012a, 2014). As in the box model studies, up to ~30 % of the O<sub>3</sub> loss in the marine boundary layer (900 < hPa) is found to be driven by halogens (Saiz-Lopez et al., 2012a, 2014). Similarly, high levels of halogen-driven O<sub>3</sub> loss are also found in the upper troposphere (350 > hPa > tropopause), with lower (10–15 %) impacts in the free troposphere (350 < hPa < 900) (Saiz-Lopez et al., 2012a, 2014).

In this paper we present a global modelling study of tropospheric iodine chemistry, using the GEOS-Chem chemical transport model. The new chemistry is described in Sect. 2. Section 3 describes the comparison of modelled iodine concentrations against observations. Then Sect. 4 describes modelled global chemical distributions by family. Impacts on O<sub>3</sub> and OH are described in Sect. 5. In Sect. 6 we consider interactions of iodine with bromine, and in Sect. 7 we look at key sensitivities of the simulation. Section 8 summarises our conclusions.

## 2 GEOS-Chem simulation

We use here the GEOS-Chem (<http://www.geos-chem.org>) chemical transport model version v9-02, with transport driven by assimilated meteorological and surface data fields (GEOS-5) from NASA's Global Modelling and Assimilation Office (GMAO). We have adapted the existing chemistry scheme which includes O<sub>X</sub>, HO<sub>X</sub>, NO<sub>X</sub>, and VOC chemistry as described recently in Mao et al. (2013), bromine chemistry (Parrella et al.,

2012), and a mass-based aerosol scheme. Stratospheric chemistry is climatologically represented based on LINOZ McLinden et al. (2000) for  $O_3$  and linearised chemistry is applied for other species with concentrations taken from the Global Modelling Initiative (GMI) as described previously Murray et al. (2012).

5 Iodine tracers ( $I_2$ , HOI, IO, OIO, HI,  $INO_2$ ,  $INO_3$ , I,  $INO$ ,  $CH_3I$ ,  $CH_2I_2$ ,  $CH_2IBr$ ,  $CH_2ICl$ ,  $I_2O_2$ ,  $I_2O_3$ ,  $I_2O_4$  and “aerosol iodine”) are included in the model. The modelled emissions, deposition, chemistry, photolysis and aerosol processes of these compounds are described below. No chemical processing of iodine species is performed in the stratosphere.

10 Notably our work differs from recent global iodine simulations (Saiz-Lopez et al., 2014) in its treatment of  $I_2O_X$  ( $X = 2, 3, 4$ ). Our “standard iodine simulation” considers the photolysis of these compounds whereas their “Base” simulation does not. This leads to our simulations having a more active iodine chemistry and this is discussed in 2.4.

15 For budgets and general analysis we run the model at  $2^\circ \times 2.5^\circ$  resolution for two years (2004–2006) discarding the 1st “spin up” year and using the final year (2005) for analysis and budgets. The model output is discussed with focus on the marine boundary layer ( $900 < hPa$ ); the free troposphere ( $350 < hPa < 900$ ); and upper troposphere ( $350 > hPa >$  tropopause). Comparisons with observations involve separate spun-up 20 simulations, run with the date appropriate meteorology, sampled at the spatially and temporally nearest grid box.

## 2.1 Iodine emissions

Both organic and inorganic iodine species (Table 1) are emitted into the atmosphere. Organic iodine compounds ( $CH_3I$ ,  $CH_2I_2$ ,  $CH_2IBr$ , and  $CH_2ICl$ ) are emitted from the monthly emissions of Ordóñez et al. (2012) which follows Bell et al. (2002) for  $CH_3I$ . Inorganic iodine compounds (HOI,  $I_2$ ), formed from the uptake of  $O_3$  to the ocean and the subsequent ocean surface reaction of  $O_3$  with iodide ( $I^-$ ), are emitted as calculated from Eqs. (19) and (20) in Carpenter et al. (2013). We parameterise ocean surface  $I^-$

## Iodine’s impact on tropospheric oxidants: a global model study in GEOS-Chem

T. Sherwen et al.

[Title Page](#)

[Abstract](#)

[Introduction](#)

[Conclusions](#)

[References](#)

[Tables](#)

[Figures](#)

[|◀](#)

[▶|](#)

[◀](#)

[▶](#)

[Back](#)

[Close](#)

[Full Screen / Esc](#)

[Printer-friendly Version](#)

[Interactive Discussion](#)



concentration from the sea surface squared temperature relationship in Table 2 from Chance et al. (2014), the O<sub>3</sub> concentration in the bottom-most level of the model, and the 10 m wind speed from metrological fields.

Global emission totals (Table 1) are consistent with recent work (Saiz-Lopez et al., 2014) for organic iodine compounds as they also use Ordóñez et al. (2012). Inorganic fluxes calculated in this study are 32 % lower in previous work (Saiz-Lopez et al., 2014), despite using the same parameterisation (Carpenter et al., 2013; MacDonald et al., 2014). Although, model specific differences exist in sea surface temperatures, 10 m wind speeds and O<sub>3</sub> concentration the largest differences lie in the choice of parameterisation for sea surface iodide (see Sect. 7.5).

## 2.2 Iodine deposition

The model's deposition scheme has recently been updated (Amos et al., 2012). Dry deposition of the new iodine compounds is computed via the standard GEOS-Chem implementation of the “resistance-in-series” approach (Wesely, 1989) using literature Henry's law coefficients (Sander, 1999). This approach is applied to I<sub>2</sub>, HI, HOI, INO<sub>2</sub>, INO<sub>3</sub>, I<sub>2</sub>O<sub>2</sub>, I<sub>2</sub>O<sub>3</sub> and I<sub>2</sub>O<sub>4</sub>. Aerosol iodine is assumed to have the same deposition properties as sulfate aerosol.

Wet deposition is calculated for I<sub>2</sub>, HI, HOI, INO<sub>2</sub>, INO<sub>3</sub>, I<sub>2</sub>O<sub>2</sub>, I<sub>2</sub>O<sub>3</sub>, and I<sub>2</sub>O<sub>4</sub> for both large scale (frontal) and convection rain by applying scavenging in and below clouds (Liu et al., 2001) using species-specific values for Henry's law coefficients (Sander, 1999; Vogt et al., 1999) and molar heats of formation (Kaltsoyannis and Plane, 2008; Sander, 1999) as shown in Table 2. Fractionation between gas and liquid on ice is considered (Parrella et al., 2012; Stuart and Jacobson, 2003). Aerosol iodine is assumed to have the same deposition properties as sulfate aerosol.

## Iodine's impact on tropospheric oxidants: a global model study in GEOS-Chem

T. Sherwen et al.

[Title Page](#)

[Abstract](#)

[Introduction](#)

[Conclusions](#)

[References](#)

[Tables](#)

[Figures](#)

[|◀](#)

[▶|](#)

[◀](#)

[▶](#)

[Back](#)

[Close](#)

[Full Screen / Esc](#)

[Printer-friendly Version](#)

[Interactive Discussion](#)



## 2.3 Iodine chemistry scheme

The gas phase iodine chemistry is shown in Tables 3 and 4. We include all iodine reactions presented by recent IUPAC (Atkinson et al., 2007, 2008) and JPL 10-6 (Sander et al., 2011) compilations relevant to the troposphere. Some additional reactions are included based on recent work (Sommariva et al., 2012; von Glasow et al., 2002) as justified in Sect. A1.1. Reactions within aerosol following uptake of species ( $\text{HI}$ ,  $\text{HOI}$ ,  $\text{INO}_2$ ,  $\text{INO}_3$ ) and processing of higher iodine oxides ( $\text{I}_2\text{O}_X$ ,  $X = 2, 3, 4$ ) after formation of  $\text{I}_2\text{O}_X$  are not treated explicitly but are parameterised as described in Sect. 2.5.

## 2.4 Photolysis rates

- Photolysis reactions are summarised in Table 5. Photolysis rates are calculated online using the standard FAST-J code implementation in GEOS-Chem (Mao et al., 2010). Cross-sections are processed to the 7 wavelength bins used by FAST-J (Bian and Prather, 2002). For most cross-sections JPL 10-6 (Sander et al., 2011) values were used. For  $\text{I}_2\text{O}_X$  ( $X = 2, 3, 4$ ) we assume the same absorption cross section as  $\text{INO}_3$ , an approach used previously (Bloss et al., 2010). For most species ( $\text{I}_2$ ,  $\text{HOI}$ ,  $\text{IO}$ ,  $\text{OIO}$ ,  $\text{INO}$ ,  $\text{INO}_2$ ,  $\text{I}_2\text{O}_2$ ,  $\text{CH}_3\text{I}$ ,  $\text{CH}_2\text{I}_2$ ,  $\text{CH}_2\text{IBr}$  and  $\text{CH}_2\text{ICl}$ ) we assume a quantum yield of 1, but for  $\text{INO}_3$  we use a quantum yield of 0.21 (Sander et al., 2011).

## 2.5 Heterogeneous processes

- In line with previous studies (McFiggans et al., 2000), we consider that the uptake of  $\text{HOI}$ ,  $\text{INO}_2$  and  $\text{INO}_3$  leads to the recycling of iodine back into the gas phase as  $\frac{1}{2}\text{I}_2$  on sea-salt aerosol alone, whereas irreversible loss via uptake of  $\text{HI}$  leads to the generation of aerosol phase iodine. Uptake of  $\text{I}_2\text{O}_X$  ( $X = 2, 3, 4$ ) also leads to the generation of aerosol phase iodine (on any aerosol). Heterogeneous uptake rates are computed using the GEOS-Chem standard code (Jacob, 2000) from reactive uptake coefficients

|  |                              |
|--|------------------------------|
| <a href="#">Title Page</a>               |                              |
| <a href="#">Abstract</a>                 | <a href="#">Introduction</a> |
| <a href="#">Conclusions</a>              | <a href="#">References</a>   |
| <a href="#">Tables</a>                   | <a href="#">Figures</a>      |
| <a href="#">◀</a>                        | <a href="#">▶</a>            |
| <a href="#">◀</a>                        | <a href="#">▶</a>            |
| <a href="#">Back</a>                     | <a href="#">Close</a>        |
| <a href="#">Full Screen / Esc</a>        |                              |
| <a href="#">Printer-friendly Version</a> |                              |
| <a href="#">Interactive Discussion</a>   |                              |

( $\gamma$ ). Reactions considered and values of  $\gamma$  used are based on recommendations and previous studies (see Table 6 and Sect. A1.2).

## 2.6 Model bromine simulation

The bromine simulation in GEOS-Chem is described in Parrella et al. (2012) and bromine chemistry is included in the “standard simulation” throughout the paper. Parrella et al. (2012) presented a range of comparisons against satellite BrO observations. Although in general the model reproduces many of the features, there is a systematic underestimation of tropospheric BrO. New aircraft observations show that tropospheric BrO (Volkamer et al., 2015; Wang et al., 2015) may be higher than within our simulation. Our simulation also underestimates surface BrO observed in the tropical Atlantic marine boundary layer ( $\text{hPa} < 900$ ) ( $\sim 2 \text{ pptv}$ , Read et al., 2008) by a ratio of  $\sim 5$  ( $0.4 \text{ pptv}$ ). We consider the uncertainty in BrO concentration on our simulation as a part of our sensitivity study in Sect. 7.

## 3 Iodine model results and observation comparisons

In this section we describe and evaluate our iodine simulation. We initially focus on observational constraints for those iodine compounds that are directly emitted (Sect. 3.1), and then on the only secondary product which has been comprehensively observed (IO) (Sect. 3.2). We then turn to the averaged distribution of modelled iodinated compounds throughout the troposphere (Sect. 4).

### 20 3.1 Emitted iodine compounds

Figures 1 and 2 show annually averaged zonal (Fig. 1) and surface concentrations (Fig. 2) of organic and inorganic iodine precursors and their degradation products. These figures clearly illustrate the oceanic nature of iodine source species ( $\text{CH}_3\text{I}$ ,  $\text{CH}_2\text{I}_2$ ,  $\text{CH}_2\text{ICl}$ ,  $\text{CH}_2\text{IBr}$ ,  $\text{HOI}$ ,  $\text{I}_2$ ), with the highest concentrations over the tropical

|  |                              |
|--|------------------------------|
| <a href="#">Title Page</a>               |                              |
| <a href="#">Abstract</a>                 | <a href="#">Introduction</a> |
| <a href="#">Conclusions</a>              | <a href="#">References</a>   |
| <a href="#">Tables</a>                   | <a href="#">Figures</a>      |
| <a href="#">◀</a>                        | <a href="#">▶</a>            |
| <a href="#">◀</a>                        | <a href="#">▶</a>            |
| <a href="#">Back</a>                     | <a href="#">Close</a>        |
| <a href="#">Full Screen / Esc</a>        |                              |
| <a href="#">Printer-friendly Version</a> |                              |
| <a href="#">Interactive Discussion</a>   |                              |

ocean. These plots also highlight the contribution of the included terrestrial CH<sub>3</sub>I paddy field source (25 %) to global CH<sub>3</sub>I concentrations from the Bell et al. (2002) emissions included in Ordóñez et al. (2012).

The emissions used here for organic iodine species have been assessed in (Ordóñez et al., 2012). We briefly present here a comparison between observations of CH<sub>3</sub>I and CH<sub>2</sub>ICl (Fig. 3) made during the UK Combined Airborne Studies in the Tropics (CAST) campaign over the tropical pacific (Guam) from January and February of 2014. These observations were made by gas chromatography mass spectrometry (GC-MS) as described in Andrews et al. (2015), using whole air samples from the Facility Airborne Atmospheric Measurement (FAAM) BAe 146-301 atmospheric research aircraft with techniques described in Andrews et al. (2013). The model shows an ability to capture the trend of decreasing concentration profile with height, but appears to underestimate the CH<sub>3</sub>I concentrations (Fig. 3). Concentrations of CH<sub>2</sub>ICl appear to be better simulated (Fig. 3). Although not definitive, this brief comparison suggests the model, if anything, underestimates the concentration of organic iodine.

The first in-situ remote open ocean I<sub>2</sub> concentration measurements were made at Cape Verde (Lawler et al., 2014). This dataset reported concentrations increasing between dusk and dawn in the range 0.2 to 1.7 pptv for the two separate measurement campaigns in May 2007 and May 2009 respectively. Our model captures the diurnal variation in I<sub>2</sub> of essentially zero during the day and increasing I<sub>2</sub> concentration during the night peaking just before dawn, but ranges between 2.5 and 7.5 pptv. Some component of this over estimate probably relates to the model's iodine heterogenous recycling which assumes 100 % conversion of HOI, NO<sub>3</sub>, and NO<sub>2</sub> into  $\frac{1}{2}$  I<sub>2</sub> rather than ICl and IBr which has been observed in laboratory studies (Braban et al., 2007).

## 25 3.2 Iodine oxide (IO) observations

Effectively, the only secondary iodine compound that has been observed and reported is IO. A comparison of a range of surface observations is shown in Fig. 4. Good agreement is seen in the West Pacific (TransBrom, Großmann et al., 2013) and tropical

[Title Page](#)[Abstract](#)[Introduction](#)[Conclusions](#)[References](#)[Tables](#)[Figures](#)[◀](#)[▶](#)[Back](#)[Close](#)[Full Screen / Esc](#)[Printer-friendly Version](#)[Interactive Discussion](#)

Atlantic at Cape Verde (Mahajan et al., 2010; Read et al., 2008), but the model has a generally high bias compared with other datasets (HALOCast-P, Mahajan et al., 2012; Malasapina, Prados-Roman et al., 2015b).

Biases between the daytime modelled and measured IO at Cape Verde and during the TransBrom cruise biases are within ~22 and ~16 % respectively. However, the model overestimates the Malasapina cruise IO concentrations (bias ~+50 to 250 %), and both under and over estimates values from the HALOCast-P cruise (bias ~−0.92 to 280 %). When all observations are latitudinally averaged (onto a 20° grid) a median bias of 66 % is found.

In Fig. 5 we show a comparison with recent aircraft IO observations from the TORERO campaign (Volkamer et al., 2015; Wang et al., 2015), which took place over the eastern Pacific. The model captures the vertical profile of IO but over estimates the observations (average bias of +82 % within the binned comparison). Biases in the comparison are greatest (bias = +125 %) in the marine boundary layer (hPa < 900) and lowest (bias = +73 %) in the free troposphere (350 < hPa < 900). The median bias in the upper troposphere (350 > hPa > tropopause) is +95 %.

From these comparisons it is evident that the model has some skill in simulating the average global surface distribution of IO (within a factor of 2) and similar skill at reproducing average vertical profiles. However, there is significant variability between locations, datasets and measurement groups. Increased global coverage, especially vertically, and inter-comparison of observational techniques are needed to better constrain the IO distribution.

#### 4 Modelled distribution of iodinated compounds

We now analyse the modelled distribution of iodinated compounds. We start with the total gas phase inorganic iodine I<sub>Y</sub> species ( $2I_2 + HOI + IO + OIO + HI + INO + INO_2 + INO_3 + 2I_2O_2 + 2I_2O_3 + 2I_2O_4$ ) and then move to the distribution of the IO<sub>X</sub> (I + IO) family.

[Title Page](#)[Abstract](#)[Introduction](#)[Conclusions](#)[References](#)[Tables](#)[Figures](#)[|◀](#)[▶|](#)[◀](#)[▶](#)[Back](#)[Close](#)[Full Screen / Esc](#)[Printer-friendly Version](#)[Interactive Discussion](#)

## 4.1 Total inorganic iodine ( $I_Y$ )

The modelled iodine system is schematically shown in Fig. 6. Iodine emissions total  $3.8 \text{ Tg I yr}^{-1}$  with most of this ( $3.2 \text{ Tg I yr}^{-1}$ ) coming from the inorganic source (84 %). This is comparable to the 83 % calculated by Prados-Roman et al. (2015b) (Ocean only,  $60^\circ \text{N}$ – $60^\circ \text{S}$ ). Most (56 %) of the emissions occur in the tropics ( $22^\circ \text{S}$  to  $22^\circ \text{N}$ ). Our emissions which include inorganic emissions, compare with reported values of  $1.8 \text{ Tg I yr}^{-1}$  (Saiz-Lopez et al., 2012a) and  $2.6 \text{ Tg I yr}^{-1}$  (Saiz-Lopez et al., 2014) which also include an inorganic source.

Previous studies that did not consider an inorganic iodine source give values of  $0.58 \text{ Tg I yr}^{-1}$  (Ordóñez et al., 2012), and  $0.65 \text{ Tg I yr}^{-1}$  (Jones et al., 2010), consistent with our organic emissions. HOI represents the single largest source of oceanic iodine (76 %) with averaged oceanic emissions of  $1.4 \times 10^8 \text{ atoms (I) cm}^{-2} \text{ s}^{-1}$ . This value is towards the lower end of flux values required to reproduce IO observations in recent box modelling studies (Großmann et al., 2013; Jones et al., 2010; Mahajan et al., 2009).

Iodine deposition is predominantly through HOI (51 %). The remainder is mostly through deposition of  $\text{INO}_3$  (20 %) and aerosol iodine formed by heterogeneous loss of gaseous iodine ( $\text{HI}$ ,  $\text{I}_2\text{O}_X$ ) (24 %). The majority of the deposition sink is back into the ocean (91 %). The global  $I_Y$  lifetime is 3.3 days but where depositional scavenging is weakest (upper troposphere,  $350 > \text{hPa} >$  tropopause) this can increase by three orders of magnitudes.

Figures 7 and 8 show the average vertical and zonal distribution of iodine compounds through the troposphere. As expected given the surface source, the concentration of iodine drops with altitude. This drop is rapid across the top of the boundary layer. The concentrations of the short-lived source gases ( $\text{CH}_2\text{IX}$  and  $\text{I}_2$ ) are negligible outside of the lowest model levels but the concentrations of others ( $\text{CH}_3\text{I}$  and HOI) persist further through the column. For  $\text{CH}_3\text{I}$  this is due to its longer lifetime of  $\sim 4$  days. However, the lifetime of HOI is shorter ( $\sim 4$  min) and its persistence at higher altitudes reflects secondary chemical sources. From the top of the boundary layer to  $\sim 10 \text{ km}$

Title Page

Abstract

Introduction

Conclusions

References

Tables

Figures

|◀

▶|

Back

Close

Full Screen / Esc

Printer-friendly Version

Interactive Discussion



## Iodine's impact on tropospheric oxidants: a global model study in GEOS-Chem

T. Sherwen et al.

[Title Page](#)

[Abstract](#)

[Introduction](#)

[Conclusions](#)

[References](#)

[Tables](#)

[Figures](#)

[|◀](#)

[▶|](#)

[◀](#)

[▶](#)

[Back](#)

[Close](#)

[Full Screen / Esc](#)

[Printer-friendly Version](#)

[Interactive Discussion](#)



## 5 Impact of iodine on O<sub>3</sub> and OH

ACPD

15, 20957–21023, 2015

O<sub>3</sub> and OH are two key parameters for climate and air quality. Previous studies (Bloss et al., 2005; Saiz-Lopez et al., 2008, 2012a) have identified significant impacts of iodine on these compounds. Here we compare our model predictions to available observational constraints and then diagnose the model change.

### 5.1 Impact on O<sub>3</sub>

On inclusion of iodine, the calculated global tropospheric O<sub>3</sub> burden drops from 367 to 334 Tg (9.0 %). Figure 9 shows the annual average tropospheric column, surface and zonal change in O<sub>3</sub>. On average the O<sub>3</sub> burdens in the marine boundary layer (900 < hPa) decreased by 19.5 %, by 9.8 % the free troposphere (350 < hPa < 900), and 6.2 % in the upper troposphere (350 > hPa > tropopause). The decrease is greater in the Southern Hemisphere (9.5 %), than the Northern Hemisphere (8.5 %).

Surface (lowest most model level) O<sub>3</sub> shows an average decrease of 3.5 ppbv globally, with large spatial variability (Fig. 10) and greater decrease over the oceans (21 %) than the land (7.3 %). Comparing against the Global Atmospheric Watch (GAW, Sofen et al., 2015) surface O<sub>3</sub> observations (Fig. 10), there is no obvious decrease in the ability of the model to capture seasonality in surface O<sub>3</sub> although there is systematic decrease in O<sub>3</sub> concentration with the inclusion of iodine.

Figure 11 shows a comparison between a selection of annually averaged O<sub>3</sub> sonde profiles for the same year (2005, World Ozone and Ultraviolet Data Centre WOUDC, 2014) and our model simulation with and without iodine. A decrease in O<sub>3</sub> concentration is evident throughout the troposphere (average of 3.1 ppbv). As with comparison of surface observations (Fig. 11), no clear decline in model skill at capturing annual sonde profiles is apparent on inclusion of iodine, with some locations improving and others degrading. An exception to this is O<sub>3</sub> observations greater than 60° S at the surface where bias are increased and in the tropical free troposphere (350 < hPa < 900) where model O<sub>3</sub> biases are decreased.

## Iodine's impact on tropospheric oxidants: a global model study in GEOS-Chem

T. Sherwen et al.

[Title Page](#)

[Abstract](#)

[Introduction](#)

[Conclusions](#)

[References](#)

[Tables](#)

[Figures](#)

[|◀](#)

[▶|](#)

[Back](#)

[Close](#)

[Full Screen / Esc](#)

[Printer-friendly Version](#)

[Interactive Discussion](#)



## 5.2 O<sub>3</sub> budget

We diagnose the impact of iodine on O<sub>3</sub> by calculating the model's tropospheric odd oxygen budget in Table 7. Here we define O<sub>X</sub> as O<sub>3</sub> + NO<sub>2</sub> + 2NO<sub>3</sub> + PAN + PMN + PPN + HNO<sub>4</sub> + 3N<sub>2</sub>O<sub>5</sub> + HNO<sub>3</sub> + BrO + HOBr + BrNO<sub>2</sub> + 2BrNO<sub>3</sub> + MPN + IO + HOI + INO<sub>2</sub> + 2INO<sub>3</sub> + 2OIO + 2I<sub>2</sub>O<sub>2</sub> + 3I<sub>2</sub>O<sub>3</sub> + 4I<sub>2</sub>O<sub>4</sub>.

Iodine provides a global tropospheric O<sub>X</sub> loss of  $\sim 750 \text{ Tg yr}^{-1}$  (15 % of the total). This is significantly larger than the  $184 \text{ Tg yr}^{-1}$  from bromine chemistry and is comparable to the sink from the O<sub>3</sub> + OH reaction. Overwhelmingly this loss is from the photolysis of HOI after its production from the reaction of IO with HO<sub>2</sub>. The O<sub>3</sub> production term increases slightly ( $\sim 1\%$ ) with the inclusion of iodine reflecting small changes in the total reactive nitrogen (NO<sub>Y</sub>) partitioning.

Iodine induced O<sub>3</sub> loss within the marine (land mask applied and between 50° N–50° S) troposphere of  $\sim 540 \text{ Tg yr}^{-1}$  is comparable to previous reported values Saiz-Lopez et al. (2014) when I<sub>2</sub>O<sub>X</sub> (X = 2,3,4) photolysis is included ( $\sim 500 \text{ Tg yr}^{-1}$ ).

Figure 12 shows the relative importance of different O<sub>X</sub> sinks in the vertical. The “classical” O<sub>3</sub> loss routes ( $h\nu + \text{H}_2\text{O}$ , HO<sub>X</sub>) dominate; however within the boundary layer and the upper troposphere (350 > hPa > tropopause), iodine represents 33 and 26 % of the total loss, respectively. The loss within the marine boundary layer (900 < hPa) in this study is again comparable to values reported recently of 28 % (Prados-Roman et al., 2015a). This decreases rapidly with increasing altitude within the lower troposphere to values closer to 10 % reflecting the lower of IO concentrations (see Figs. 7 and 8). In the upper troposphere, higher IO<sub>X</sub> and BrO<sub>X</sub> concentrations lead to increased loss of O<sub>3</sub>.

Figure 13 shows the zonal variation in the different O<sub>X</sub> destruction terms (in terms of the O<sub>X</sub> lifetime). It is evident that, in the model, iodine destruction is more spatially prevalent than bromine destruction, which is confined predominantly to the Southern Ocean. The impact of iodine is hemispherically asymmetric reflecting the higher NO<sub>X</sub> in the Northern Hemisphere, higher BrO concentrations in the southern oceans and the

Title Page

Abstract

Introduction

Conclusions

References

Tables

Figures

|◀

▶|

◀

▶|

Back

Close

Full Screen / Esc

Printer-friendly Version

Interactive Discussion

larger ocean area in the Southern Hemisphere increasing emissions. Convective transport in the tropics rapidly lifts iodine species into the free troposphere ( $350 < \text{hPa} < 900$ ) where they can destroy  $\text{O}_3$ .

### 5.3 Impact on OH

- 5 Previous box model studies which investigated impact of iodine on OH concentration in the Antarctic (Saiz-Lopez et al., 2008), mid-latitude coastal (Bloss, 2005), tropical marine regions (Mahajan et al., 2010), and the free troposphere (Wang et al., 2015) found increases in the OH concentration due to IO enhancing conversion of  $\text{HO}_2$  to OH. However we find that the inclusion of iodine in the model has little impact on the global mean  
10 OH concentrations. It slightly increases from  $12.2$  to  $12.5 \times 10^5 \text{ molec.cm}^{-3}$  (1.8 %). This small increase is surprising given the 12 % reduction in the primary source ( $\text{O}_3 + \text{H}_2\text{O} + h\nu$ ) due to lower  $\text{O}_3$  concentrations. However, this is to some extent, compensated for by an increase in the rate of conversion of  $\text{HO}_2$  to OH by IO. Previous  
15 studies using constrained box models (Bloss, 2005; Saiz-Lopez et al., 2008) could not consider this impact on the primary production of OH and it appears from our simulation that the overall impact is lower than previously thought.

## 6 Combined impact of bromine and iodine

- 20 The importance of halogen cross-over reactions ( $\text{BrO} + \text{IO}$ ) for  $\text{O}_3$  loss has been previously highlighted and found to be required to replicate observed diurnal surface  $\text{O}_3$  loss in the marine boundary layer (Read et al., 2008). To explore these interactions a further two runs were performed: one simulation with iodine but without bromine ("just iodine") and one without any halogens ("no hal").

25 Global tropospheric burdens of are 390, 367 (reduction of 5.9 %), 357 (8.5 %) and 334 Tg (14 %) for the simulations without halogens ("no ha"), with just bromine ("standard simulation"), with just iodine ("just iodine"), and with both iodine and bromine

|  |                              |
|--|------------------------------|
| <a href="#">Title Page</a>               |                              |
| <a href="#">Abstract</a>                 | <a href="#">Introduction</a> |
| <a href="#">Conclusions</a>              | <a href="#">References</a>   |
| <a href="#">Tables</a>                   | <a href="#">Figures</a>      |
| <a href="#">◀</a>                        | <a href="#">▶</a>            |
| <a href="#">◀</a>                        | <a href="#">▶</a>            |
| <a href="#">Back</a>                     | <a href="#">Close</a>        |
| <a href="#">Full Screen / Esc</a>        |                              |
| <a href="#">Printer-friendly Version</a> |                              |
| <a href="#">Interactive Discussion</a>   |                              |

chemistry (“iodine simulation”) respectively. The sum of the changes in O<sub>3</sub> burden for the runs considering halogens individually is very slightly lower (0.1 %) than when considered simultaneously.

Figure 14 shows the combined daily surface loss rate of O<sub>3</sub> driven by bromine and iodine (upper panel). This correlates with IO concentrations (Fig. 2) reflecting iodine’s role in marine boundary layer O<sub>3</sub> destruction. Figure 14 also shows modelled and observed fractional diurnal fractional O<sub>3</sub> change at Cape Verde in the remote marine boundary layer (lower panel). The diurnal change is calculated by subtracting each day’s maximum O<sub>3</sub> mixing ratio from hourly observations (2006–2012, Sofen et al., 2015). Each value is then divided by the mean value for that day to give a fractional change, then this is presented averaged by hour over all the observations. The simulation’s fidelity increases significantly with the inclusion of iodine (Fig. 14) but there is little impact from bromine. Whereas modelled IO concentrations at Cape Verde shows agreement with observations (Fig. 4), BrO concentrations (~ 0.4 pptv) are significantly lower than reported (~ 2 pptv, Read et al., 2008). This underestimate of BrO in the model is a systemic problem (see Sect. 2.6) and so model estimates of the impact of Br on atmospheric composition described here are probably an underestimate.

Global mean tropospheric concentrations of OH are 12.80, 12.24, 13.02, and  $12.47 \times 10^5$  molecules cm<sup>-3</sup> for the simulations without halogens (“no hal”), with just bromine (“standard simulation”), with just iodine (“just iodine”), and with both iodine and bromine chemistry (“iodine simulation”) respectively. OH shows a differing response to bromine and iodine chemistry. As discussed in Sect. 5.3, inclusion of iodine leads to a small increase in OH concentrations. When solely iodine is considered, OH concentrations increase by 1.8 % compared to when no halogens are included. Whereas bromine chemistry leads to a reduction in OH (4.3 %), as reported previously (Parrella et al., 2012), due to enhanced production by HOBr photolysis not compensating for a decrease in the primary OH source (O<sub>3</sub> + H<sub>2</sub>O + hν) from a reduced O<sub>3</sub> burden. The net impact overall on inclusion of halogens is a global reduction in OH (2.6 %).

## Iodine’s impact on tropospheric oxidants: a global model study in GEOS-Chem

T. Sherwen et al.

[Title Page](#)

[Abstract](#)

[Introduction](#)

[Conclusions](#)

[References](#)

[Tables](#)

[Figures](#)

[|◀](#)

[▶|](#)

[◀](#)

[▶](#)

[Back](#)

[Close](#)

[Full Screen / Esc](#)

[Printer-friendly Version](#)

[Interactive Discussion](#)



In our simulations, the global impact of Br and I chemistry are essentially additive with apparently limited impact from the cross reactions. The global impact of iodine appears significantly larger than that of bromine, however, given that the model underestimates the concentrations of Br compounds this should be subject to future study.

## 5 7 Sensitivity studies

As discussed in the introduction, a range of uncertainties exist in our understanding of tropospheric iodine. We perform sensitivity analysis on some of these parameters using the  $4^\circ \times 5^\circ$  version of the model. We chose to analyse the sensitivity to inclusion of inorganic iodine emissions, heterogeneous loss and cycling, photolysis rates and 10 ocean surface iodide. Values are quoted as a % change from the iodine simulation described in Sects. 2–5. Figure 16 summarises the fractional impact of these experiments on the globally averaged vertical distribution of  $I_Y$ ,  $O_3$  and vertical profile comparison of observations of IO from the TORERO campaign (Volkamer et al., 2015; Wang et al., 2015). Additional information is listed in Table A1 in the Appendix A.

### 15 7.1 Just Organic Iodine

Until recently many studies solely considered organic iodine (Jones et al., 2010; Ordóñez et al., 2012) emissions. As discussed in Sect. 3.1, our simulation uses the Carpenter et al. (2013) inorganic emission parameterisation as well as organic iodine emissions from Ordóñez et al. (2012). When we just consider organic iodine 20 emissions (“Just org. I”) we find that global  $I_Y$  burdens decrease ( $\sim 65\%$ ), and mean surface marine boundary layer ( $900 < hPa$ ) IO decreases ( $\sim 83\%$ ). The median bias against TORERO IO observations decreases by  $\sim 68\%$  and becomes a negative bias of  $-25\%$ . The decreased  $I_Y$  leads to the mean global OH decreasing by  $0.64\%$  and global tropospheric  $O_3$  increasing by  $5.5\%$ .

|  |                              |
|--|------------------------------|
| <a href="#">Title Page</a>               |                              |
| <a href="#">Abstract</a>                 | <a href="#">Introduction</a> |
| <a href="#">Conclusions</a>              | <a href="#">References</a>   |
| <a href="#">Tables</a>                   | <a href="#">Figures</a>      |
| <a href="#">◀</a>                        | <a href="#">▶</a>            |
| <a href="#">◀</a>                        | <a href="#">▶</a>            |
| <a href="#">Back</a>                     | <a href="#">Close</a>        |
| <a href="#">Full Screen / Esc</a>        |                              |
| <a href="#">Printer-friendly Version</a> |                              |
| <a href="#">Interactive Discussion</a>   |                              |

## 7.2 Heterogeneous uptake and cycling

There is limited experimental data for the reaction probability ( $\gamma$ ) for iodine species on aerosol. Our base case scheme follows the literature precedent (McFiggans et al., 2000) and assumes heterogeneous recycling of unity (e.g. HOI =  $\frac{1}{2}$  I<sub>2</sub>) on sea salt which is not limited by aerosol acidity. However, the acidity of aerosol may limit iodine cycling as not all sea-salt aerosols are acidic (Alexander, 2005) and other aerosols may irreversibly uptake iodine. Detail on the reaction probabilities ( $\gamma$ ) chosen is in Appendix A. To explore these uncertainties four simulations were run: (1) with the  $\gamma$  values that led to I<sub>2</sub> release doubled ("het. cycle  $\times 2$ "), (2) with the  $\gamma$  values halved ("het. cycle /2"), (3) with all uptake reactions leading to a net loss of iodine ("No het. cycle"), and (4) a run where sulfate aerosol leads to a sink for iodine with the same  $\gamma$  values as for sea salt ("Sulfate uptake").

Increasing the heterogeneous cycling ("het. cycle  $\times 2$ ") converts more HOI (the dominant I<sub>Y</sub> species) into I<sub>2</sub>, thus reducing the rate of HOI deposition. The global I<sub>Y</sub> burden increases by ~ 6 %, mean surface marine boundary layer (900 < hPa) IO concentration increases by ~ 2 % and the median bias with respect to the TORERO IO observations increases by ~ 26 to 100 % (Fig. 16). Decreasing the heterogeneous cycling ("het. cycle /2") has the opposite impact of roughly the same magnitude. Global average I<sub>Y</sub> burden decreases (~ 4.3 %), average surface marine boundary layer IO decreases (~ 1.8 %) and the median bias with respect to the TORERO IO observations decreases (~ 18 %) to 66 %.

The impacts of these changes is small overall. Increased iodine cycling leads to a decrease in the tropospheric O<sub>3</sub> burden of ~ 0.69 % and global mean OH increases by ~ 0.05 %, whereas decreased cycling leads to the tropospheric O<sub>3</sub> burden increasing by ~ 0.56 % and OH decreasing by ~ 0.09 %.

By removing the release of I<sub>2</sub> to the gas-phase following uptake of iodine ("no het. cycle") or by considering irreversible iodine loss to sulfate aerosol ("Sulfate uptake") the global I<sub>Y</sub> burdens decrease significantly by 47 and 48 %, respectively. Surface marine

|  |                              |
|--|------------------------------|
| <a href="#">Title Page</a>               |                              |
| <a href="#">Abstract</a>                 | <a href="#">Introduction</a> |
| <a href="#">Conclusions</a>              | <a href="#">References</a>   |
| <a href="#">Tables</a>                   | <a href="#">Figures</a>      |
| <a href="#">◀</a>                        | <a href="#">▶</a>            |
| <a href="#">◀</a>                        | <a href="#">▶</a>            |
| <a href="#">Back</a>                     | <a href="#">Close</a>        |
| <a href="#">Full Screen / Esc</a>        |                              |
| <a href="#">Printer-friendly Version</a> |                              |
| <a href="#">Interactive Discussion</a>   |                              |

[Title Page](#)[Abstract](#)[Introduction](#)[Conclusions](#)[References](#)[Tables](#)[Figures](#)[|](#)[|](#)[◀](#)[▶](#)[Back](#)[Close](#)[Full Screen / Esc](#)[Printer-friendly Version](#)[Interactive Discussion](#)

boundary layer ( $900 < hPa$ ) IO concentration decreases by 48 and 22 %. The median bias with respect to the TORERO IO observations decreases in the case of “no het. cycle” (~ 84 %) to 13 % and decreases in “Sulfate uptake” (~ 92 %) to –6.7 %. The “Sulfate uptake” scenario shifts the median bias with the TORERO IO observations to be negative, instead of positive (~ +80 % for the base iodine simulation at  $4 \times 5$ ).  
5

This large decrease in  $I_Y$  decreases the potency of iodine chemistry. The reductions in the tropospheric  $O_3$  burdens (4.1 and 4.5 % for “no het. cycle” and “Sulfate uptake”) are comparable to the simulation where only organic iodine sources are considered (5.5 %, “Just I Org.”). Global mean OH decreases slightly by ~ 0.54 and ~ 0.87 % under these two scenarios. These two sensitivity runs represent large perturbations to the iodine system, highlighting the importance and uncertainties in heterogeneous chemistry.  
10  
15

### 7.3 Uncertainties in photolysis parameters

Absorption cross-sections and quantum yields for iodine species are few and their temperature dependencies are not known. Notably, the absorption cross sections for the higher iodine oxides ( $I_2O_2$ ,  $I_2O_3$ ,  $I_2O_4$ ) are highly uncertain (Bloss et al., 2001; Gómez Martín et al., 2005; Spietz et al., 2005) and we use the  $INO_3$  spectrum in our simulation. This uncertainty was tested in 3 simulations: (1) absorption cross-sections were doubled (“ $I_2O_X$  X-sections  $\times 2$ ”), (2) tentative literature assignments of spectra were used for  $I_2O_3$  and  $I_2O_2$  (Bloss et al., 2001; Gómez Martín et al., 2005; Spietz et al., 2005), with  $I_2O_2$  used for  $I_2O_4$ , (3) and finally no  $I_2O_X$  photolysis at all was considered (“No  $I_2O_X$  photolysis”).  
20  
25

Sensitivity runs “ $I_2O_X$  X-sections  $\times 2$ ” and “ $I_2O_X$  exp. X-sections” increase photolysis rates, therefore resulting in an increase in the  $I_Y$  lifetime of 5.3 and 8.3 % and the  $I_Y$  burdens by 3.1 and 4.8 % respectively. The average surface marine boundary layer ( $900 < hPa$ ) IO concentration responds by increasing by 4.3 and 6.7 % for “ $I_2O_X$  X-sections  $\times 2$ ” and “ $I_2O_X$  exp. X-sections” respectively. Both these simulation increase median bias with TORERO IO observations by ~ 4.8 to 84 % and ~ 7.6 to 86 %, re-

spectively. The impacts on  $O_3$  burden are small with a decrease of 0.4 and 0.6 % for “ $I_2O_X$  X-sections  $\times 2$ ” and “ $I_2O_X$  exp. X-sections” respectively. Global mean OH concentrations increase by 0.05 and 0.09 % respectively.

The removal of  $I_2O_X$  ( $X = 2, 3, 4$ ) photolysis reduces the global tropospheric  $I_Y$  burden (~35 %), reduces surface marine boundary layer ( $900 < hPa$ ) IO (~40 %), increases tropospheric  $O_3$  burden (5.1 %) and decreases global mean OH (0.9 %) with respect to the base iodine simulation. The median bias with respect to the TORERO IO observations becomes negative and decreases by ~81 to 16 %, illustrating a large change in the simulated IO profile by removing the  $I_2O_X$  photolysis (Fig. 16). This was also noted by Prados-Roman et al. (2015b) with respect to surface observations.

Our “No  $I_2O_X$  photolysis” simulation is akin to the “base” simulation of (Saiz-Lopez et al., 2014). This was presented as a lower bounds for iodine chemistry. Their “ $Jl_XO_Y$ ” simulation is akin to our iodine simulation. Saiz-Lopez et al. (2014) find a decrease in marine tropospheric  $O_3$  column burden of 3.0 and 6.1 % compared to a simulation with no iodine chemistry for their “base” and “ $Jl_XO_Y$ ” simulations respectively. Considering the same domain our comparable simulations show values of 4.0 to 8.7 %.

## 7.4 Marine boundary layer BrO concentration

As discussed in the introduction and Sect. 6, bromine and iodine chemistry are coupled. GEOS-Chem appears to underestimate BrO (Parrella et al., 2012), with for example, our simulation underestimating the BrO concentrations at Cape Verde (Read et al., 2008) (~2 pptv) by a factor of ~5.

To test the sensitivity of the model to BrO concentrations, a simulation with BrO concentration fixed at 2 pptv in the daytime marine boundary layer was run (“MBL BrO 2 pptv”). Increased BrO leads to increased OIO concentrations ( $BrO + IO \rightarrow OIO + Br$ , R15), which leads to increased higher oxide production which in turn increases  $I_Y$  loss and decreases  $I_Y$  burden (10 %). The median bias in vertical comparisons with TORERO IO observations decreases by ~12 to 71 %. Although the overall tropospheric  $O_3$  burden decreases by 3.7 %, the average  $O_3$  change at the surface is larger

[Title Page](#)[Abstract](#)[Introduction](#)[Conclusions](#)[References](#)[Tables](#)[Figures](#)[|◀](#)[▶|](#)[◀](#)[▶](#)[Back](#)[Close](#)[Full Screen / Esc](#)[Printer-friendly Version](#)[Interactive Discussion](#)

and shows a decrease of ~8 % (Fig. 16) which is the largest decrease in O<sub>3</sub> found within these sensitivity simulations.

## 7.5 Ocean surface iodide (I<sup>-</sup>) concentration

Chance et al. (2014) compiled the available ocean surface iodide (I<sup>-</sup>) observations and investigated correlations with various environmental parameters. They found that ocean surface iodide correlated most strongly with the square of sea surface temperature, as used in this work. However MacDonald et al. (2014), using a sub-set of the Chance et al. (2014) data, found that an Arrhenius parameterisation gave best agreement. Figure 15 shows annual averaged ocean surface iodide generated from both parameterisations. The sea surface temperatures are taken from the annual mean GEOS field used in GEOS-Chem. The area weighted mean concentrations are 37.6 and 80.8 nM for MacDonald et al. (2014) and Chance et al. (2014), respectively. Both approaches reproduce the latitudinal gradient observed in Fig. 1 of Chance et al. (2014), however large discrepancies are apparent in magnitude. The dataset reported in Chance et al. (2014) has a median value of 77 nM and interquartile range of 28–140 nM.

Inclusion of the MacDonald et al. (2014) iodide parameterisation (“Ocean Iodide”) reduces the inorganic iodine flux by 51 % to 1.9 Tg, which in turn decreases the global tropospheric iodine I<sub>T</sub> burden (23 %) and surface IO concentrations (34 %). The median bias in comparison with TORERO vertical profiles decreases by ~47 to 42 %. Tropospheric O<sub>3</sub> burden increases by 2.1 % and global mean OH increase by 0.17 % with respect to the iodine simulation.

## 7.6 Higher oxide lifetime

Within the model we have considered the uptake of the I<sub>2</sub>O<sub>X</sub> ( $X = 2, 3, 4$ ) to aerosol as an irreversible loss of iodine, with the same reactive probability ( $\gamma$ ) as INO<sub>2</sub> (0.02).

[Title Page](#)[Abstract](#)[Introduction](#)[Conclusions](#)[References](#)[Tables](#)[Figures](#)[|◀](#)[▶|](#)[◀](#)[▶](#)[Back](#)[Close](#)[Full Screen / Esc](#)[Printer-friendly Version](#)[Interactive Discussion](#)

We assess our sensitivity to this assumption by running simulations doubling (“ $I_2O_X(\gamma) \times 2$ ”) and halving this value (“ $I_2O_X(\gamma)/2$ ”).

The effect of doubling  $\gamma$  leads to decreasing global tropospheric  $I_Y$  burden (5.1 %), decreasing surface marine boundary layer ( $900 < hPa$ ) IO (4.6 %), and decreases the 5 median bias in vertical comparisons with TORERO IO ( $\sim 6.9\%$ ) to 75 %. This leads to a slightly increased global tropospheric  $O_3$  burden (0.54 %), and marginally decrease in global mean OH (0.08 %). The effect of halving  $\gamma$  is essentially symmetrical, with an increased global tropospheric  $I_Y$  burden (4.3 %), increased surface marine boundary layer ( $900 < hPa$ ) IO concentration (4.3 %), and an increased median bias in vertical 10 comparisons with TORERO IO by  $\sim 4.4$  to 84 %. This leads to slightly decreased global tropospheric  $O_3$  burden (0.44 %), and marginally increase in OH (0.05 %).

## 7.7 Summary

Uncertainties in the atmospheric chemistry of iodine lead to some significant uncertainties on iodine's impact of atmospheric composition. Further laboratory studies on the 15 photolytic properties of high oxides would reduce uncertainty, as would a more detailed understanding of the rates of heterogenous cycling on a range of aerosols. The interplay between bromine and iodine chemistry is also potentially significant for the oxidant budgets. Given the inorganic iodine emission's role as the largest source of iodine into the atmosphere, improved constraints on the concentration of oceanic iodide would 20 also reduce uncertainties. It is clear that we do not have a complete understanding of iodine chemistry in the atmosphere and further laboratory and field observations are necessary to provide a stronger constraint.

## 8 Conclusions

We have implemented a representation of the tropospheric chemistry of iodine into the 25 GEOS-Chem model and compared it against a range of observational datasets. We

Title Page

Abstract

Introduction

Conclusions

References

Tables

Figures

◀

▶

Back

Close

Full Screen / Esc

Printer-friendly Version

Interactive Discussion



estimate a global emission of  $3.8 \text{ Tg yr}^{-1}$  of iodine, which is consistent with previous work. We find this dominated by the inorganic ocean source (84 %), and the majority (91 %) of deposition is back to the oceans.

Comparisons with the limited IO observational dataset shows that the model is within a factor of 2 of the observations on average. Iodine reduces the global tropospheric  $\text{O}_3$  burden by ~9 %. Global mean OH concentrations are increased (1.8 %) by the presence of iodine due to the reduction in the  $\text{O}_3\text{-H}_2\text{O}$  primary source being compensated for by an increased conversion of  $\text{HO}_2$  into OH via the photolysis of HOI. Both changes involve HOI production and destruction cycles.

Our understanding of iodine chemistry is hampered by limited laboratory studies of both its gas and aerosol phase chemistry, by limited field measurements of atmospheric iodine compounds and poor understanding of ocean surface iodide and its chemistry. Impacts on  $\text{O}_3$  and OH are sensitive to the uncertainty of ocean iodine emissions, the parameterisation of iodine recycling in aerosol, to the photolysis parameters for the higher oxides and to the assumed Br chemistry. Given its role as the largest component of atmospheric iodine, and its central role in both  $\text{O}_3$  destruction and  $\text{HO}_2$  to IO cycling, a priority should be given to instrumentation to measure HOI.

## Appendix A:

### A1 Additional details on sensitivity runs

#### A1.1 Details of reactions within scheme, but not present within IUPAC/JPL

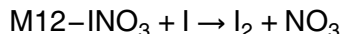
The field of iodine chemistry is still young, and some reactions that are used within box model/global studies are not in the IUPAC/JPL compilations due to uncertainties in the laboratory studies or for other reasons. Differences choices have been made regarding reactions included in previous box model (Bloss et al., 2010; Mahajan et al., 2009; Read et al., 2008; Saiz-Lopez et al., 2008; Sommariva et al., 2012) and global

[Title Page](#)[Abstract](#)[Introduction](#)[Conclusions](#)[References](#)[Tables](#)[Figures](#)[|◀](#)[▶|](#)[Back](#)[Close](#)[Full Screen / Esc](#)[Printer-friendly Version](#)[Interactive Discussion](#)

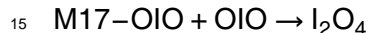
model studies (Breider, 2010; Ordóñez et al., 2012; Saiz-Lopez et al., 2012b, 2014). The following reactions have been included within our simulation's chemistry scheme (Tables 3 and 4) although they are not in the IUPAC/JPL compilations.



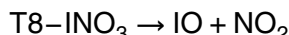
- 5 Uncertainties exist over product channels for this reaction (Sommariva et al., 2012). In our study we assume the products are IO and H<sub>2</sub>O based on laboratory experiments (Riffault et al., 2005) and previous box model analysis (Sommariva et al., 2012). It is not included within JPL/IUPAC compilations.



- 10 This reaction's rate is based on a single theoretical study (Kaltsoyannis and Plane, 2008), and it is thus not included within either the JPL or IUPAC compilations. The impact of inclusion within a box model was found to be minimal, except in high iodine and NOx conditions (Sommariva et al., 2012). It is argued that this reaction rate needs determination with higher accuracy (Sommariva et al., 2012).



This reaction rate is from a single experimental study (Gómez Martín et al., 2007), which yielded a lower limit at  $1.2 \pm 0.3 \times 10^{-10} \text{ cm}^3 \text{ molec}^{-1} \text{ s}^{-1}$ . This reaction is not included within JPL/IUPAC compilations. This reaction is included in this work, along with the reverse reaction (Reaction T12, I<sub>2</sub>O<sub>4</sub> → 2OIO).



Good consensus exists between reaction rates (298 K) for the forward reaction (Reaction T7) from JPL ( $7.68 \times 10^{-31} \text{ cm}^3 \text{ molec}^{-1} \text{ s}^{-1}$ ) and IUPAC ( $7.96 \times$

|  |                              |
|--|------------------------------|
| <a href="#">Title Page</a>               |                              |
| <a href="#">Abstract</a>                 | <a href="#">Introduction</a> |
| <a href="#">Conclusions</a>              | <a href="#">References</a>   |
| <a href="#">Tables</a>                   | <a href="#">Figures</a>      |
| <a href="#">◀</a>                        | <a href="#">▶</a>            |
| <a href="#">◀</a>                        | <a href="#">▶</a>            |
| <a href="#">Back</a>                     | <a href="#">Close</a>        |
| <a href="#">Full Screen / Esc</a>        |                              |
| <a href="#">Printer-friendly Version</a> |                              |
| <a href="#">Interactive Discussion</a>   |                              |

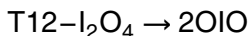
$10^{-31} \text{ cm}^3 \text{ molec}^{-1} \text{ s}^{-1}$ ). The reverse reaction (Reaction T8) is included in the IUPAC (Atkinson et al., 2007) without direct experiment observation. No recommendation is given in the recent recent JPL compilation (Sander et al., 2011). The  $\text{INO}_3$  thermal stability used by studies has led to magnitude of differences between reaction rates (298 K) from  $1.08 \times 10^{-2}$  (Read et al., 2008) to  $2.51 \times 10^{-5} \text{ cm}^3 \text{ molec}^{-1} \text{ s}^{-1}$  (Sommariva et al., 2012). The latter uses the most recent theoretical study (Kaltsoyannis and Plane, 2008), which we also use here. The forward reaction (Reaction T7) has been included ubiquitously in iodine modelling work; and reverse reaction (Reaction T8) is employed in the majority of, but not all studies (Ordóñez et al., 2012). Both reactions are included in this work.



A single experimental study (Gómez Martín et al., 2007) gives a upper and lower rate of  $1.5 \times 10^{-10}$  and  $1.5 \times 10^{-11} \text{ cm}^3 \text{ molec}^{-1} \text{ s}^{-1}$ , respectively. We use the higher value in this work as in others (Saiz-Lopez et al., 2008; Sommariva et al., 2012). The rate was found to increase with pressure over the range studied (10–400 hPa, Gómez Martín et al., 2007), suggesting greater importance at the higher pressures found at the surface.



These reaction has been studied solely theoretically (Kaltsoyannis and Plane, 2008) and are not included in JPL/IUPAC compilations. A temperature dependent rate was calculated theoretically using the Rice–Ramsperger–Kassel–Markus theory (Ordóñez et al., 2012) which is used in our work.



The rate is calculated from the value for binding energy of the dimer (Kaltsoyannis and Plane, 2008), and is not included in JPL/IUPAC compilations. Considering that we have included reaction M17 ( $\text{OIO} + \text{OIO} \rightarrow \text{I}_2\text{O}_4$ ), we also include the reverse Reaction T12 in our work at the Kaltsoyannis and Plane (2008) rate.

[Title Page](#)[Abstract](#)[Introduction](#)[Conclusions](#)[References](#)[Tables](#)[Figures](#)[|◀](#)[▶|](#)[◀](#)[▶](#)[Back](#)[Close](#)[Full Screen / Esc](#)[Printer-friendly Version](#)[Interactive Discussion](#)

## A1.2 Detail of reactive uptake coefficients ( $\gamma$ ) used for heterogeneous reactions

As described in Sect. 3.1, we stoichiometrically emit  $I_2$  following uptake of species that hydrolyse to HOI ( $INO_2$ ,  $INO_3$ , HOI). We assume this to avoid double counting of  $Br_2$  release already included within the model as described by Parrella et al. (2012). Lack of, or limited experimental data reduces certainty on heterogeneous processing of halogens. The reactive uptake coefficients ( $\gamma$ ) used in this study are experimentally constrained wherever possible or follow previously estimated values in the literature as described below.

The JPL compilation notes a single experimental study of HOI uptake on  $H_2SO_4$ , yielding mass accommodation coefficients ( $\alpha$ ) in the range 0.02 to 0.07 (Sander et al., 2011). Another two studies on ice and salt are reported in JPL 10-6 with lower limits of > 0.0022 and > 0.01 respectively (Sander et al., 2011). IUPAC evaluates two experimental studies which “concur (the) uptake coefficient is large”, but no recommendation is given due to possible uncertainties in reversibility (Crowley et al., 2010). The  $\gamma$  values used in literature range between 0.01 (Mahajan et al., 2009; Breider, 2010) and 0.5 (Saiz-Lopez et al., 2007). The higher end of this range originates from an investigation of the sensitivity to this parameter within THAMO by Saiz-Lopez et al. (2007) for which the basecase was set as 0.02. A  $\gamma$  value of 0.02 is used within our work.

For  $INO_2$  and  $INO_3$  no experiment work is available on the uptake and values have previously been estimated by analogy with measured equivalent bromine species. For  $INO_3$  a  $\gamma$  value of 0.01 has been frequently used based on estimations (Mahajan et al., 2009; Ordóñez et al., 2012), but values have been used up to 0.2 (Bloss et al., 2010). For  $INO_2$   $\gamma$  values of 0.01 (Mahajan et al., 2009) or 0.02 (Ordóñez et al., 2012; Saiz-Lopez et al., 2007) have often been used, but  $\gamma$  values up to 0.1 have also been used (Bloss et al., 2010). In this work  $\gamma$  values of 0.01 and 0.02 are used for  $INO_3$  and  $INO_2$  respectively.

|  |                              |
|--|------------------------------|
| <a href="#">Title Page</a>               |                              |
| <a href="#">Abstract</a>                 | <a href="#">Introduction</a> |
| <a href="#">Conclusions</a>              | <a href="#">References</a>   |
| <a href="#">Tables</a>                   | <a href="#">Figures</a>      |
| <a href="#">◀</a>                        | <a href="#">▶</a>            |
| <a href="#">◀</a>                        | <a href="#">▶</a>            |
| <a href="#">Back</a>                     | <a href="#">Close</a>        |
| <a href="#">Full Screen / Esc</a>        |                              |
| <a href="#">Printer-friendly Version</a> |                              |
| <a href="#">Interactive Discussion</a>   |                              |

**Iodine's impact on tropospheric oxidants: a global model study in GEOS-Chem**

T. Sherwen et al.

[Title Page](#)[Abstract](#)[Introduction](#)[Conclusions](#)[References](#)[Tables](#)[Figures](#)[|◀](#)[▶|](#)[◀](#)[▶](#)[Back](#)[Close](#)[Full Screen / Esc](#)[Printer-friendly Version](#)[Interactive Discussion](#)

The IUPAC compilation includes a recommendation for HI uptake  $\gamma$  on ice of 0.2 (Crowley et al., 2010), based on three experimental studies. A  $\gamma$  value of 0.1 has most often been used in modelling studies (Breider, 2010; Mahajan et al., 2009; Saiz-Lopez et al., 2008) and is used in this work.

- For  $I_2O_X$  ( $X = 2, 3, 4$ ) no experimental data is available for reactive uptake coefficients. The uptake has been discussed in the literature, including a box model study which tested sensitivity around a base value of 0.02 (Saiz-Lopez et al., 2008). The  $\gamma$  value for  $I_2O_X$  was set at 0.02 by analogy  $INO_2$ . This value is highly uncertain and values up to 1 have been used for gamma in modelling studies (Bloss et al., 2010).
- A value of 0.02 is used within this work.

**Acknowledgements.** R. Volkamer acknowledges funding from US National Science Foundation CAREER award ATM-0847793, AGS-1104104, and AGS-1452317. The involvement of the NSF-sponsored Lower Atmospheric Observing Facilities, managed and operated by the National Center for Atmospheric Research (NCAR) Earth Observing Laboratory (EOL), is acknowledged.

T. Sherwen would like to acknowledge constructive comments from and conversations with all coauthors as well as R. Chance and J. Schmidt.

This work was funded by NERC quota studentship NE/K500987/1 with support from the NERC BACCHUS and CAST projects NE/L01291X/1, NE/J006165/1.

**References**

- Ainsworth, E. A., Yendrek, C. R., Sitch, S., Collins, W. J., and Emberson, L. D.: The effects of tropospheric ozone on net primary productivity and implications for climate change, *Annu. Rev. Plant Bio.*, 63, 637–661, doi:10.1146/annurev-arplant-042110-103829, 2012. 20960
- Alexander, B.: Sulfate formation in sea-salt aerosols: Constraints from oxygen isotopes, *J. Geophys. Res.*, 110, D10307, doi:10.1029/2004JD005659, 2005. 20979
- Amos, H. M., Jacob, D. J., Holmes, C. D., Fisher, J. A., Wang, Q., Yantosca, R. M., Corbett, E. S., Galarneau, E., Rutter, A. P., Gustin, M. S., Steffen, A., Schauer, J. J., Graydon, J. A., Louis, V. L. St., Talbot, R. W., Edgerton, E. S., Zhang, Y., and Sunderland, E. M.:

Gas-particle partitioning of atmospheric Hg(II) and its effect on global mercury deposition, *Atmos. Chem. Phys.*, 12, 591–603, doi:10.5194/acp-12-591-2012, 2012. 20967

Andrews, S. J., Jones, C. E., and Carpenter, L. J.: Aircraft measurements of very short-lived halocarbons over the tropical Atlantic Ocean, *Geophys. Res. Lett.*, 40, 1005–1010, doi:10.1002/grl.50141, 2013. 20970

Andrews, S. J., Hackenberg, S. C., and Carpenter, L. J.: Technical Note: A fully automated purge and trap GC-MS system for quantification of volatile organic compound (VOC) fluxes between the ocean and atmosphere, *Ocean Sci.*, 11, 313–321, doi:10.5194/os-11-313-2015, 2015. 20970

10 Atkinson, R.: Atmospheric chemistry of VOCs and NO<sub>x</sub>, *Atmos. Environ.*, 34, 2063–2101, doi:10.1016/S1352-2310(99)00460-4, 2000. 20960

Atkinson, R., Baulch, D. L., Cox, R. A., Hampson, R. F., Kerr, J. A., Rossi, M. J., and Troe, J.: Evaluated kinetic and photochemical data for atmospheric chemistry: Supplement VIII, halogen species – IUPAC Subcommittee on gas kinetic data evaluation for atmospheric chemistry, *J. Phys. Chem. Ref. Data*, 29, 167–266, doi:10.1063/1.556058, 2000. 20961

15 Atkinson, R., Baulch, D. L., Cox, R. A., Crowley, J. N., Hampson, R. F., Hynes, R. G., Jenkin, M. E., Rossi, M. J., and Troe, J.: Evaluated kinetic and photochemical data for atmospheric chemistry: Volume III – gas phase reactions of inorganic halogens, *Atmos. Chem. Phys.*, 7, 981–1191, doi:10.5194/acp-7-981-2007, 2007. 20961, 20968, 20986, 21001, 21002

20 Atkinson, R., Baulch, D. L., Cox, R. A., Crowley, J. N., Hampson, R. F., Hynes, R. G., Jenkin, M. E., Rossi, M. J., Troe, J., and Wallington, T. J.: Evaluated kinetic and photochemical data for atmospheric chemistry: Volume IV – gas phase reactions of organic halogen species, *J. Phys. Chem. Ref. Data*, 8, 4141–4496, 2008. 20968, 21001

25 Bedjanian, Y., Le Bras, G., and Poulet, G.: Kinetic study of the Br + IO, I + BrO and Br + I<sub>2</sub> reactions. Heat of formation of the BrO radical, *Chem. Phys. Lett.*, 266, 233–238, doi:10.1016/S0009-2614(97)01530-3, 1997. 21001

30 Bell, N., Hsu, L., Jacob, D. J., Schultz, M. G., Blake, D. R., Butler, J. H., King, D. B., Lobert, J. M., and Maier-Reimer, E.: Methyl iodide: atmospheric budget and use as a tracer of marine convection in global models, *J. Geophys. Res.-Atmos.*, 107, ACH 8–1–ACH 8–12, doi:10.1029/2001jd001151, 2002. 20966, 20970

Iodine's impact on tropospheric oxidants: a global model study in GEOS-Chem

T. Sherwen et al.

[Title Page](#)

[Abstract](#)

[Introduction](#)

[Conclusions](#)

[References](#)

[Tables](#)

[Figures](#)

◀

▶

[Back](#)

[Close](#)

[Full Screen / Esc](#)

[Printer-friendly Version](#)

[Interactive Discussion](#)



## Iodine's impact on tropospheric oxidants: a global model study in GEOS-Chem

T. Sherwen et al.

[Title Page](#)

[Abstract](#)

[Introduction](#)

[Conclusions](#)

[References](#)

[Tables](#)

[Figures](#)

[|◀](#)

[▶|](#)

[◀](#)

[▶](#)

[Back](#)

[Close](#)

[Full Screen / Esc](#)

[Printer-friendly Version](#)

[Interactive Discussion](#)

Bian, H. S. and Prather, M. J.: Fast-J2: accurate simulation of stratospheric photolysis in global chemical models, *J. Atmos. Chem.*, 41, 281–296, doi:10.1023/a:1014980619462, 2002. 20968

Bloss, W. J.: Impact of halogen monoxide chemistry upon boundary layer OH and HO<sub>2</sub> concentrations at a coastal site, *Geophys. Res. Lett.*, 32, L06814, doi:10.1029/2004GL022084, 2005. 20964, 20976

Bloss, W. J., Rowley, D. M., Cox, R. A., and Jones, R. L.: Kinetics and products of the IO self-reaction, *J. Phys. Chem. A*, 105, 7840–7854, doi:10.1021/jp0044936, 2001. 20980

Bloss, W. J., Evans, M. J., Lee, J. D., Sommariva, R., Heard, D. E., and Pilling, M. J.: The oxidative capacity of the troposphere: coupling of field measurements of OH and a global chemistry transport model, *Faraday Discuss.*, 130, 425–436, doi:10.1039/b419090d, 2005. 20974

Bloss, W. J., Camredon, M., Lee, J. D., Heard, D. E., Plane, J. M. C., Saiz-Lopez, A., Bauguitte, S. J.-B., Salmon, R. A., and Jones, A. E.: Coupling of HO<sub>x</sub>, NO<sub>x</sub> and halogen chemistry in the antarctic boundary layer, *Atmos. Chem. Phys.*, 10, 10187–10209, doi:10.5194/acp-10-10187-2010, 2010. 20968, 20984, 20987, 20988

Braban, C. F., Adams, J. W., Rodriguez, D., Cox, R. A., Crowley, J. N., and Schuster, G.: Heterogeneous reactions of HOI, ICl and IBr on sea salt and sea salt proxies, *Phys. Chem. Chem. Phys.*, 9, 3136–3148, doi:10.1039/b700829e, 2007. 20970

Breider, T. J.: Coupled Halogen-Sulfur-Aerosol Modelling in a 3D Chemical Transport Model, PhD thesis, University of Leeds, Leeds, 2010. 20985, 20987, 20988

Butz, A., Bösch, H., Camy-Peyret, C., Chipperfield, M. P., Dorf, M., Kreycy, S., Kritten, L., Prados-Román, C., Schwärzle, J., and Pfeilsticker, K.: Constraints on inorganic gaseous iodine in the tropical upper troposphere and stratosphere inferred from balloon-borne solar occultation observations, *Atmos. Chem. Phys.*, 9, 7229–7242, doi:10.5194/acp-9-7229-2009, 2009. 20962, 20964

Carpenter, L. J., MacDonald, S. M., Shaw, M. D., Kumar, R., Saunders, R. W., Parthipan, R., Wilson, J., and Plane, J. M. C.: Atmospheric iodine levels influenced by sea surface emissions of inorganic iodine, *Nat. Geosci.*, 6, 108–111, doi:10.1038/ngeo1687, 2013. 20961, 20966, 20967, 20978

Chameides, W. L. and Davis, D. D.: Iodine: its possible role in tropospheric photochemistry, *J. Geophys. Res.-Oceans*, 85, 7383–7398, doi:10.1029/JC085iC12p07383, 1980. 20960, 20964

- Chance, R., Baker, A. R., Carpenter, L., and Jickells, T. D.: The distribution of iodide at the sea surface, *Environ. Sci.: Processes Impacts*, 16, 1841–1859, doi:10.1039/C4EM00139G, 2014. 20963, 20967, 20982, 21022
- 5 Chuck, A. L., Turner, S. M., and Liss, P. S.: Oceanic distributions and air-sea fluxes of biogenic halocarbons in the open ocean, *J. Geophys. Res.-Oceans*, 110, C10022, doi:10.1029/2004jc002741, 2005. 20961
- Crowley, J. N., Ammann, M., Cox, R. A., Hynes, R. G., Jenkin, M. E., Mellouki, A., Rossi, M. J., Troe, J., and Wallington, T. J.: Evaluated kinetic and photochemical data for atmospheric chemistry: Volume V – heterogeneous reactions on solid substrates, *Atmos. Chem. Phys.*, 10, 9059–9223, doi:10.5194/acp-10-9059-2010, 2010. 20987, 20988, 21004
- 10 Dix, B., Baidar, S., Bresch, J., Hall, S., Schmidt, K., Wang, S.-Y., and Volkamer, R.: Detection of iodine monoxide in the tropical free troposphere, *P. Natl. Acad. Sci. USA*, 110, 2035–2040, doi:10.1073/pnas.1212386110, 2013. 20962, 20964
- 15 Fiore, A. M., Naik, V., Spracklen, D. V., Steiner, A., Unger, N., Prather, M., Bergmann, D., Cameron-Smith, P. J., Cionni, I., Collins, W. J., Dalsoren, S., Eyring, V., Folberth, G. A., Ginoux, P., Horowitz, L. W., Josse, B., Lamarque, J.-F., MacKenzie, I. A., Nagashima, T., O'Connor, F. M., Righi, M., Rumbold, S. T., Shindell, D. T., Skeie, R. B., Sudo, K., Szopa, S., Takemura, T., and Zeng, G.: Global air quality and climate, *Chem. Soc. Rev.*, 41, 6663–6683, doi:10.1039/C2CS35095E, 2012. 20960
- 20 Fowler, D., Amann, M., Anderson, R., Ashmore, M., Cox, P., Depledge, M., Derwent, D., Grennfelt, P., Hewitt, N., Hov, O., Jenkin, M., Kelly, F., Liss, P., Pilling, M., Pyle, J., Slingo, J., and Stevenson, D.: Ground-level ozone in the 21st century: future trends, impacts and policy implications, *Tech. rep.*, The Royal Society, 2008. 20960
- Garland, J. A. and Curtis, H.: Emission of iodine from the sea surface in the presence of ozone, *J. Geophys. Res.*, 86, 3183–3186, doi:10.1029/JC086iC04p03183, 1981. 20961
- 25 Gómez Martín, J. C., Spietz, P., and Burrows, J. P.: Spectroscopic studies of the  $I_2/O_3$  photochemistry: Part 1: Determination of the absolute absorption cross sections of iodine oxides of atmospheric relevance, *J. Photoch. Photobio. A*, 176, 15–38, doi:10.1016/j.jphotochem.2005.09.024, 2005. 20980
- 30 Gómez Martín, J. C., Spietz, P., and Burrows, J. P.: Kinetic and mechanistic studies of the  $I_2/O_3$  photochemistry, *J. Phys. Chem. A*, 111, 306–320, doi:10.1021/jp061186c, 2007. 20985, 20986, 21001, 21002

**Iodine's impact on tropospheric oxidants: a global model study in GEOS-Chem**

T. Sherwen et al.

[Title Page](#)[Abstract](#)[Introduction](#)[Conclusions](#)[References](#)[Tables](#)[Figures](#)[|◀](#)[▶|](#)[◀](#)[▶](#)[Back](#)[Close](#)[Full Screen / Esc](#)[Printer-friendly Version](#)[Interactive Discussion](#)

- Gómez Martín, J. C., Mahajan, A. S., Hay, T. D., Prados-Roman, C., Ordonez, C., MacDonald, S. M., Plane, J. M. C., Sorribas, M., Gil, M., Mora, J. F. P., Reyes, M. V. A., Oram, D. E., Leedham, E., and Saiz-Lopez, A.: Iodine chemistry in the eastern Pacific marine boundary layer, *J. Geophys. Res.-Atmos.*, 118, 887–904, doi:10.1002/jgrd.50132, 2013. 20963, 20964
- 5 Großmann, K., Frieß, U., Peters, E., Wittrock, F., Lampel, J., Yilmaz, S., Tschritter, J., Sommariva, R., von Glasow, R., Quack, B., Krüger, K., Pfeilsticker, K., and Platt, U.: Iodine monoxide in the Western Pacific marine boundary layer, *Atmos. Chem. Phys.*, 13, 3363–3378, doi:10.5194/acp-13-3363-2013, 2013. 20962, 20963, 20964, 20970, 20972, 21011
- 10 Jacob, D. J.: Heterogeneous chemistry and tropospheric ozone, *Atmos. Environ.*, 34, 2131–2159, doi:10.1016/S1352-2310(99)00462-8, 2000. 20968
- Jones, C. E., Hornsby, K. E., Sommariva, R., Dunk, R. M., Von Glasow, R., McFiggans, G., and Carpenter, L. J.: Quantifying the contribution of marine organic gases to atmospheric iodine, *Geophys. Res. Lett.*, 37, L18804, doi:10.1029/2010gl043990, 2010. 20961, 20962, 20963, 20972, 20978
- 15 Kaltsoyannis, N. and Plane, J. M. C.: Quantum chemical calculations on a selection of iodine-containing species ( $\text{IO}$ ,  $\text{OIO}$ ,  $\text{INO}_3$ ,  $(\text{IO})_2$ ,  $\text{I}_2\text{O}_3$ ,  $\text{I}_2\text{O}_4$  and  $\text{I}_2\text{O}_5$ ) of importance in the atmosphere, *Phys. Chem. Chem. Phys.*, 10, 1723–1733, 2008. 20967, 20985, 20986, 21000, 21001, 21002
- 20 Kim, K.-H., Shon, Z.-H., Nguyen, H. T., and Jeon, E.-C.: A review of major chlorofluorocarbons and their halocarbon alternatives in the air, *Atmos. Environ.*, 45, 1369–1382, doi:10.1016/j.atmosenv.2010.12.029, 2011. 20960
- 25 Law, K. S. and Sturges, W. T.: Scientific Assessment of Ozone Depletion, 2006 Chapter 2: Halogenated Very Short-Lived Substances, Tech. rep., 2006. 20961
- Lawler, M. J., Mahajan, A. S., Saiz-Lopez, A., and Saltzman, E. S.: Observations of  $\text{I}_2$  at a remote marine site, *Atmos. Chem. Phys.*, 14, 2669–2678, doi:10.5194/acp-14-2669-2014, 2014. 20962, 20963, 20970
- 30 Lelieveld, J. and Dentener, F. J.: What controls tropospheric ozone?, *J. Geophys. Res.-Atmos.*, 105, 3531–3551, doi:10.1029/1999JD901011, 2000. 20960
- Liu, H., Jacob, D. J., Bey, I., and Yantosca, R. M.: Constraints from  $^{210}\text{Pb}$  and  $^{7}\text{Be}$  on wet deposition and transport in a global three-dimensional chemical tracer model driven by assimilated meteorological fields, *J. Geophys. Res.-Atmos.*, 106, 12109–12128, doi:10.1029/2000JD900839, 2001. 20967

## Iodine's impact on tropospheric oxidants: a global model study in GEOS-Chem

T. Sherwen et al.

[Title Page](#)

[Abstract](#)

[Introduction](#)

[Conclusions](#)

[References](#)

[Tables](#)

[Figures](#)

◀

▶

◀

▶

[Back](#)

[Close](#)

[Full Screen / Esc](#)

[Printer-friendly Version](#)

[Interactive Discussion](#)

MacDonald, S. M., Gómez Martín, J. C., Chance, R., Warriner, S., Saiz-Lopez, A., Carpenter, L. J., and Plane, J. M. C.: A laboratory characterisation of inorganic iodine emissions from the sea surface: dependence on oceanic variables and parameterisation for global modelling, *Atmos. Chem. Phys.*, 14, 5841–5852, doi:10.5194/acp-14-5841-2014, 2014. 20961, 20967, 20982, 21022

Mahajan, A. S., Oetjen, H., Saiz-Lopez, A., Lee, J. D., McFiggans, G. B., and Plane, J. M. C.: Reactive iodine species in a semi-polluted environment, *Geophys. Res. Lett.*, 36, L16803, doi:10.1029/2009GL038018, 2009. 20963, 20964, 20972, 20984, 20987, 20988

Mahajan, A. S., Plane, J. M. C., Oetjen, H., Mendes, L., Saunders, R. W., Saiz-Lopez, A., Jones, C. E., Carpenter, L. J., and McFiggans, G. B.: Measurement and modelling of tropospheric reactive halogen species over the tropical Atlantic Ocean, *Atmos. Chem. Phys.*, 10, 4611–4624, doi:10.5194/acp-10-4611-2010, 2010. 20962, 20963, 20964, 20971, 20976, 21011

Mahajan, A. S., Gómez Martín, J. C., Hay, T. D., Royer, S.-J., Yvon-Lewis, S., Liu, Y., Hu, L., Prados-Roman, C., Ordóñez, C., Plane, J. M. C., and Saiz-Lopez, A.: Latitudinal distribution of reactive iodine in the Eastern Pacific and its link to open ocean sources, *Atmos. Chem. Phys.*, 12, 11609–11617, doi:10.5194/acp-12-11609-2012, 2012. 20962, 20971, 21011

Mao, J., Jacob, D. J., Evans, M. J., Olson, J. R., Ren, X., Brune, W. H., Clair, J. M. St., Crounse, J. D., Spencer, K. M., Beaver, M. R., Wennberg, P. O., Cubison, M. J., Jimenez, J. L., Fried, A., Weibring, P., Walega, J. G., Hall, S. R., Weinheimer, A. J., Cohen, R. C., Chen, G., Crawford, J. H., McNaughton, C., Clarke, A. D., Jaeglé, L., Fisher, J. A., Yantosca, R. M., Le Sager, P., and Carouge, C.: Chemistry of hydrogen oxide radicals ( $\text{HO}_x$ ) in the Arctic troposphere in spring, *Atmos. Chem. Phys.*, 10, 5823–5838, doi:10.5194/acp-10-5823-2010, 2010. 20968

Mao, J., Paulot, F., Jacob, D. J., Cohen, R. C., Crounse, J. D., Wennberg, P. O., Keller, C. A., Hudman, R. C., Barkley, M. P., and Horowitz, L. W.: Ozone and organic nitrates over the eastern United States: sensitivity to isoprene chemistry, *J. Geophys. Res.-Atmos.*, 118, 11256–11268, doi:10.1002/jgrd.50817, 2013. 20965

McFiggans, G., Plane, J. M. C., Allan, B. J., Carpenter, L. J., Coe, H., and O'Dowd, C.: A modeling study of iodine chemistry in the marine boundary layer, *J. Geophys. Res.-Atmos.*, 105, 14371–14385, doi:10.1029/1999JD901187, 2000. 20963, 20968, 20979

McFiggans, G., Bale, C. S. E., Ball, S. M., Beames, J. M., Bloss, W. J., Carpenter, L. J., Dorsey, J., Dunk, R., Flynn, M. J., Furneaux, K. L., Gallagher, M. W., Heard, D. E.,

Title Page

Abstract

Introduction

Conclusions

References

Tables

Figures

|◀

▶|

◀

▶

Back

Close

Full Screen / Esc

Printer-friendly Version

Interactive Discussion



## Iodine's impact on tropospheric oxidants: a global model study in GEOS-Chem

T. Sherwen et al.

Hollingsworth, A. M., Hornsby, K., Ingham, T., Jones, C. E., Jones, R. L., Kramer, L. J., Langridge, J. M., Leblanc, C., LeCrane, J.-P., Lee, J. D., Leigh, R. J., Longley, I., Mahajan, A. S., Monks, P. S., Oetjen, H., Orr-Ewing, A. J., Plane, J. M. C., Potin, P., Shillings, A. J. L., Thomas, F., von Glasow, R., Wada, R., Whalley, L. K., and Whitehead, J. D.: Iodine-mediated coastal particle formation: an overview of the Reactive Halogens in the Marine Boundary Layer (RHaMBLe) Roscoff coastal study, *Atmos. Chem. Phys.*, 10, 2975–2999, doi:10.5194/acp-10-2975-2010, 2010. 20963, 20964

McLinden, C. A., Olsen, S. C., Hannegan, B., Wild, O., Prather, M. J., and Sundet, J.: Stratospheric ozone in 3-D models: a simple chemistry and the cross-tropopause flux, *J. Geophys. Res.*, 105, 14653, doi:10.1029/2000JD900124, 2000. 20966

Murray, B. J., Haddrell, A. E., Peppe, S., Davies, J. F., Reid, J. P., O'Sullivan, D., Price, H. C., Kumar, R., Saunders, R. W., Plane, J. M. C., Umo, N. S., and Wilson, T. W.: Glass formation and unusual hygroscopic growth of iodic acid solution droplets with relevance for iodine mediated particle formation in the marine boundary layer, *Atmos. Chem. Phys.*, 12, 8575–8587, doi:10.5194/acp-12-8575-2012, 2012. 20966

Ordóñez, C., Lamarque, J.-F., Tilmes, S., Kinnison, D. E., Atlas, E. L., Blake, D. R., Sousa Santos, G., Brasseur, G., and Saiz-Lopez, A.: Bromine and iodine chemistry in a global chemistry-climate model: description and evaluation of very short-lived oceanic sources, *Atmos. Chem. Phys.*, 12, 1423–1447, doi:10.5194/acp-12-1423-2012, 2012. 20963, 20965, 20966, 20967, 20970, 20972, 20978, 20985, 20986, 20987, 21002

Parrella, J. P., Jacob, D. J., Liang, Q., Zhang, Y., Mickley, L. J., Miller, B., Evans, M. J., Yang, X., Pyle, J. A., Theys, N., and Van Roozendael, M.: Tropospheric bromine chemistry: implications for present and pre-industrial ozone and mercury, *Atmos. Chem. Phys.*, 12, 6723–6740, doi:10.5194/acp-12-6723-2012, 2012. 20965, 20967, 20969, 20977, 20981, 20987

Prados-Roman, C., Cuevas, C. A., Fernandez, R. P., Kinnison, D. E., Lamarque, J.-F., and Saiz-Lopez, A.: A negative feedback between anthropogenic ozone pollution and enhanced ocean emissions of iodine, *Atmos. Chem. Phys.*, 15, 2215–2224, doi:10.5194/acp-15-2215-2015, 2015a. 20963, 20975

Prados-Roman, C., Cuevas, C. A., Hay, T., Fernandez, R. P., Mahajan, A. S., Royer, S.-J., Galí, M., Simó, R., Dachs, J., Großmann, K., Kinnison, D. E., Lamarque, J.-F., and Saiz-Lopez, A.: Iodine oxide in the global marine boundary layer, *Atmos. Chem. Phys.*, 15, 583–593, doi:10.5194/acp-15-583-2015, 2015b. 20963, 20964, 20971, 20972, 20981, 21011

[Title Page](#)

[Abstract](#)

[Introduction](#)

[Conclusions](#)

[References](#)

[Tables](#)

[Figures](#)

[◀](#)

[▶](#)

[Back](#)

[Close](#)

[Full Screen / Esc](#)

[Printer-friendly Version](#)

[Interactive Discussion](#)

- Puentedura, O., Gil, M., Saiz-Lopez, A., Hay, T., Navarro-Comas, M., Gómez-Pelaez, A., Cuevas, E., Iglesias, J., and Gomez, L.: Iodine monoxide in the north subtropical free troposphere, *Atmos. Chem. Phys.*, 12, 4909–4921, doi:10.5194/acp-12-4909-2012, 2012. 20962
- Read, K. A., Mahajan, A. S., Carpenter, L. J., Evans, M. J., Faria, B. V. E., Heard, D. E., Hopkins, J. R., Lee, J. D., Moller, S. J., Lewis, A. C., Mendes, L., McQuaid, J. B., Oetjen, H., Saiz-Lopez, A., Pilling, M. J., and Plane, J. M. C.: Extensive halogen-mediated ozone destruction over the tropical Atlantic Ocean, *Nature*, 453, 1232–1235, doi:10.1038/nature07035, 2008. 20962, 20963, 20964, 20969, 20971, 20976, 20977, 20981, 20984, 20986, 21011
- Riffault, V., Bedjanian, Y., and Poulet, G.: Kinetic and mechanistic study of the reactions of OH with IBr and HOI, *J. Photoch. Photobio. A*, 176, 155–161, doi:10.1016/j.jphotochem.2005.09.002, 2005. 20985, 21001
- Saiz-Lopez, A., Plane, J. M. C., McFiggans, G., Williams, P. I., Ball, S. M., Bitter, M., Jones, R. L., Hongwei, C., and Hoffmann, T.: Modelling molecular iodine emissions in a coastal marine environment: the link to new particle formation, *Atmos. Chem. Phys.*, 6, 883–895, doi:10.5194/acp-6-883-2006, 2006. 20963
- Saiz-Lopez, A., Chance, K., Liu, X., Kurosu, T. P., and Sander, S. P.: First observations of iodine oxide from space, *Geophys. Res. Lett.*, 34, L12812, doi:10.1029/2007gl030111, 2007. 20963, 20987
- Saiz-Lopez, A., Plane, J. M. C., Mahajan, A. S., Anderson, P. S., Bauguitte, S. J.-B., Jones, A. E., Roscoe, H. K., Salmon, R. A., Bloss, W. J., Lee, J. D., and Heard, D. E.: On the vertical distribution of boundary layer halogens over coastal Antarctica: implications for  $O_3$ ,  $HO_x$ ,  $NO_x$  and the Hg lifetime, *Atmos. Chem. Phys.*, 8, 887–900, doi:10.5194/acp-8-887-2008, 2008. 20974, 20976, 20984, 20986, 20988
- Saiz-Lopez, A., Lamarque, J.-F., Kinnison, D. E., Tilmes, S., Ordóñez, C., Orlando, J. J., Conley, A. J., Plane, J. M. C., Mahajan, A. S., Sousa Santos, G., Atlas, E. L., Blake, D. R., Sander, S. P., Schaufler, S., Thompson, A. M., and Brasseur, G.: Estimating the climate significance of halogen-driven ozone loss in the tropical marine troposphere, *Atmos. Chem. Phys.*, 12, 3939–3949, doi:10.5194/acp-12-3939-2012, 2012a. 20963, 20965, 20972, 20974
- Saiz-Lopez, A., Plane, J. M. C., Baker, A. R., Carpenter, L. J., von Glasow, R., Martin, J. C. G., McFiggans, G., and Saunders, R. W.: Atmospheric chemistry of iodine, *Chem. Rev.*, 112, 1773–1804, doi:10.1021/cr200029u, 2012b. 20961, 20962, 20964, 20985
- Saiz-Lopez, A., Fernandez, R. P., Ordóñez, C., Kinnison, D. E., Gómez Martín, J. C., Lamarque, J.-F., and Tilmes, S.: Iodine chemistry in the troposphere and its effect on ozone, *Atmos.*

[Title Page](#)[Abstract](#)[Introduction](#)[Conclusions](#)[References](#)[Tables](#)[Figures](#)[|◀](#)[▶|](#)[Back](#)[Close](#)[Full Screen / Esc](#)[Printer-friendly Version](#)[Interactive Discussion](#)

5 Sander, R.: Compilation of Henry's Law Constants for Inorganic and Organic Species of Potential Importance in Environmental Chemistry, available at: <http://www.henrys-law.org> (last access: 1 January 2013), 1999. 20967, 21000

Sander, R., Vogt, R., Harris, G. W., and Crutzen, P. J.: Modelling the chemistry of ozone, halogen compounds, and hydrocarbons in the arctic troposphere during spring, Tellus B, 49, 522–532, doi:10.1034/j.1600-0889.49.issue5.8.x, 1997. 20963

10 Sander, S. P., Golden, D. M., Kurylo, M. J., Moortgat, G. K., Wine, P. H., Ravishankara, A. R., Kolb, C. E., Molina, M. J., Finlayson-Pitts, B. J., Huie, R. E., and Orkin, V. L.: Chemical kinetics and photochemical data for use, in: Atmospheric Studies Evaluation, Number 15, 2006. 21000

15 Sander, S. P., Friedl, R. R., Abbatt, J. P. D., Barker, J. R., Burkholder, J. B., Golden, D. M., Kolb, C. E., Kurylo, M. J., Moortgat, G. K., Wine, P. H., Huie, R. E., and Orkin, V. L.: Chemical kinetics and photochemical data for use in atmospheric studies, Evaluation Number 17, Tech. rep., NASA Jet Propulsion Laboratory, 2011. 20961, 20968, 20986, 20987, 21001, 21003, 21004

20 Schönhardt, A., Richter, A., Wittrock, F., Kirk, H., Oetjen, H., Roscoe, H. K., and Burrows, J. P.: Observations of iodine monoxide columns from satellite, Atmos. Chem. Phys., 8, 637–653, doi:10.5194/acp-8-637-2008, 2008. 20962

25 Shaw, M. D. and Carpenter, L. J.: Modification of ozone deposition and I<sub>2</sub> emissions at the air-aqueous interface by dissolved organic carbon of marine origin, Environ. Sci. Technol., 47, 10947–10954, doi:10.1021/es4011459, 2013. 20963

Sofen, E. D. and Evans, M. J.: Surface O<sub>3</sub> dataset, Earth Syst. Sci. Data Discuss., in preparation, 2015. 20974, 20977, 21017

20 Sommariva, R., Bloss, W. J., and von Glasow, R.: Uncertainties in gas-phase atmospheric iodine chemistry, Atmos. Environ., 57, 219–232, doi:10.1016/j.atmosenv.2012.04.032, 2012. 20961, 20962, 20968, 20984, 20985, 20986

30 Spietz, P., Gómez Martín, J. C., and Burrows, J. P.: Spectroscopic studies of the I<sub>2</sub>/O<sub>3</sub> photochemistry: Part 2. Improved spectra of iodine oxides and analysis of the IO absorption spectrum, J. Photoch. Photobio. A, 176, 50–67, doi:10.1016/j.jphotochem.2005.08.023, 2005. 20980

Iodine's impact on tropospheric oxidants: a global model study in GEOS-Chem

T. Sherwen et al.

Title Page

Abstract

Introduction

Conclusions

References

Tables

Figures

◀

▶

Back

Close

Full Screen / Esc

Printer-friendly Version

Interactive Discussion

Stuart, A. L. and Jacobson, M. Z.: A timescale investigation of volatile chemical retention during hydrometeor freezing: nonrime freezing and dry growth riming without spreading, *J. Geophys. Res.*, 108, 4178, doi:10.1029/2001JD001408, 2003. 20967

Vogt, R., Sander, R., Von Glasow, R., and Crutzen, P. J.: Iodine chemistry and its role in halogen activation and ozone loss in the marine boundary layer: a model study, *J. Atmos. Chem.*, 32, 375–395, doi:10.1023/a:1006179901037, 1999. 20967, 21000

Volkamer, R., Baidar, S., Campos, T. L., Coburn, S., DiGangi, J. P., Dix, B., Eloranta, E. W., Koenig, T. K., Morley, B., Ortega, I., Pierce, B. R., Reeves, M., Sinreich, R., Wang, S., Zondlo, M. A., and Romashkin, P. A.: Aircraft measurements of BrO, IO, glyoxal, NO<sub>2</sub>, H<sub>2</sub>O, O<sub>2</sub>–O<sub>2</sub> and aerosol extinction profiles in the tropics: comparison with aircraft-/ship-based in situ and lidar measurements, *Atmos. Meas. Tech.*, 8, 2121–2148, doi:10.5194/amt-8-2121-2015, 2015. 20962, 20963, 20964, 20969, 20971, 20978, 21012, 21023

von Glasow, R., Sander, R., Bott, A., and Crutzen, P. J.: Modeling halogen chemistry in the marine boundary layer 2. Interactions with sulfur and the cloud-covered MBL, *J. Geophys. Res.-Atmos.*, 107, 4323, doi:10.1029/2001JD000943, 2002. 20968

von Glasow, R., von Kuhlmann, R., Lawrence, M. G., Platt, U., and Crutzen, P. J.: Impact of reactive bromine chemistry in the troposphere, *Atmos. Chem. Phys.*, 4, 2481–2497, doi:10.5194/acp-4-2481-2004, 2004. 20960

Voulgarakis, A., Naik, V., Lamarque, J.-F., Shindell, D. T., Young, P. J., Prather, M. J., Wild, O., Field, R. D., Bergmann, D., Cameron-Smith, P., Cionni, I., Collins, W. J., Dalsøren, S. B., Doherty, R. M., Eyring, V., Faluvegi, G., Folberth, G. A., Horowitz, L. W., Josse, B., MacKenzie, I. A., Nagashima, T., Plummer, D. A., Righi, M., Rumbold, S. T., Stevenson, D. S., Strode, S. A., Sudo, K., Szopa, S., and Zeng, G.: Analysis of present day and future OH and methane lifetime in the ACCMIP simulations, *Atmos. Chem. Phys.*, 13, 2563–2587, doi:10.5194/acp-13-2563-2013, 2013. 20960

Wang, S.-Y., Schmidt, J., Baidar, S., Coburn, S., Dix, B., Koenig, T., Apel, E., Bowdalo, D., Campos, T., Eloranta, E., Evans, M., DiGangi, J., Zondlo, M., Gao, R.-S., Haggerty, J., Hall, S., Hornbrook, R., Jacob, D., Morley, B., Pierce, B., Reeves, M., Romashkin, P., ter Schure, A., and Volkamer, R.: Active and widespread halogen chemistry in the tropical and subtropical free troposphere, *P. Natl. Acad. Sci. USA*, 112, 9281–9286, doi:10.1073/pnas.1505142112, 2015. 20962, 20963, 20964, 20969, 20971, 20976, 20978, 21012, 21023

## Iodine's impact on tropospheric oxidants: a global model study in GEOS-Chem

T. Sherwen et al.

[Title Page](#)

[Abstract](#)

[Introduction](#)

[Conclusions](#)

[References](#)

[Tables](#)

[Figures](#)

[|◀](#)

[▶|](#)

[◀](#)

[▶](#)

[Back](#)

[Close](#)

[Full Screen / Esc](#)

[Printer-friendly Version](#)

[Interactive Discussion](#)



**Iodine's impact on tropospheric oxidants: a global model study in GEOS-Chem**

T. Sherwen et al.

[Title Page](#)[Abstract](#)[Introduction](#)[Conclusions](#)[References](#)[Tables](#)[Figures](#)[|◀](#)[▶|](#)[◀](#)[▶](#)[Back](#)[Close](#)[Full Screen / Esc](#)[Printer-friendly Version](#)[Interactive Discussion](#)

Wesely, M. L.: Parameterization of surface resistances to gaseous dry deposition in regional-scale numerical models, *Atmos. Environ.*, 23, 1293–1304, doi:10.1016/0004-6981(89)90153-4, 1989. 20967

WOUDC: WOUDC Ozone Monitoring Community, World Meteorological Organization-Global Atmosphere Watch Program (WMO-GAW)/World Ozone and Ultraviolet Radiation Data Centre (WOUDC) [Data], doi:10.14287/10000001, available at: <http://www.woudc.org>, last access: 1 October 2014. 20974, 21018

Young, P. J., Archibald, A. T., Bowman, K. W., Lamarque, J.-F., Naik, V., Stevenson, D. S., Tilmes, S., Voulgarakis, A., Wild, O., Bergmann, D., Cameron-Smith, P., Cionni, I., Collins, W. J., Dalsøren, S. B., Doherty, R. M., Eyring, V., Faluvegi, G., Horowitz, L. W., Josse, B., Lee, Y. H., MacKenzie, I. A., Nagashima, T., Plummer, D. A., Righi, M., Rumbold, S. T., Skeie, R. B., Shindell, D. T., Strode, S. A., Sudo, K., Szopa, S., and Zeng, G.: Pre-industrial to end 21st century projections of tropospheric ozone from the Atmospheric Chemistry and Climate Model Intercomparison Project (ACCMIP), *Atmos. Chem. Phys.*, 13, 2063–2090, doi:10.5194/acp-13-2063-2013, 2013. 20960, 21005

**Iodine's impact on tropospheric oxidants: a global model study in GEOS-Chem**

T. Sherwen et al.

**Table 1.** Total simulated emissions for iodinated species. Values are given as annual totals in Tg of iodine.

| Species                        | Emissions<br>Tg yr <sup>-1</sup> |
|--------------------------------|----------------------------------|
| CH <sub>3</sub> I              | 0.26                             |
| CH <sub>2</sub> I <sub>2</sub> | 0.11                             |
| CH <sub>2</sub> ICl            | 0.18                             |
| CH <sub>2</sub> IBr            | 0.05                             |
| I <sub>2</sub>                 | 0.32                             |
| HOI                            | 2.91                             |
| Total                          | 3.83                             |

## Iodine's impact on tropospheric oxidants: a global model study in GEOS-Chem

T. Sherwen et al.

**Table 2.** Henry's law coefficients and molar heats of formation of iodine species. Where Henry's law constant equals infinity a very large values is used within the model ( $1 \times 10^{20}$ ). For  $\text{I}_2\text{O}_X$  ( $X = 2, 3, 4$ ) a Henry's law constant of infinity is assumed by analogy with  $\text{INO}_3$ .

| Num. | Species                | Henry's Law Constant<br>Matm <sup>-1</sup> | Reference          | Molar Heat of Formation<br>298 K/R (K) | Reference                     |
|------|------------------------|--|--------------------|--|-------------------------------|
| D1   | HOI                    | $1.53 \times 10^4$                         | Sander (1999)      | $-8.37 \times 10^3$                    | Sander et al. (2006)          |
| D2   | HI                     | $2.50 \times 10^1$                         | Sander (1999)      | $-3.19 \times 10^3$                    | Sander et al. (2006)          |
| D3   | $\text{INO}_3$         | $\infty$                                   | Vogt et al. (1999) | $-3.98 \times 10^4$                    | Kaltsoyannis and Plane (2008) |
| D4   | $\text{I}_2\text{O}_2$ | $\infty$                                   | see caption text   | $-1.89 \times 10^4$                    | Kaltsoyannis and Plane (2008) |
| D5   | $\text{I}_2$           | $2.63 \times 10^0$                         | Sander (1999)      | $-7.51 \times 10^3$                    | Sander et al. (2006)          |
| D6   | $\text{INO}_2$         | $3.00 \times 10^{-1}$                      | Vogt et al. (1999) | $-7.24 \times 10^3$                    | Sander et al. (2006)          |
| D7   | $\text{I}_2\text{O}_3$ | $\infty$                                   | see caption text   | $-7.70 \times 10^3$                    | Kaltsoyannis and Plane (2008) |
| D8   | $\text{I}_2\text{O}_4$ | $\infty$                                   | see caption text   | $-1.34 \times 10^4$                    | Kaltsoyannis and Plane (2008) |

[Title Page](#)

[Abstract](#)

[Introduction](#)

[Conclusions](#)

[References](#)

[Tables](#)

[Figures](#)

[|◀](#)

[▶|](#)

[◀](#)

[▶](#)

[Back](#)

[Close](#)

[Full Screen / Esc](#)

[Printer-friendly Version](#)

[Interactive Discussion](#)

**Table 3.** Bimolecular iodine reactions. These are given in the Arrhenius form with the rate equal to  $A \cdot \exp(\frac{E_a}{RT})$ . Unknown values are represented by a dash and these set to zero in the model, reducing the exponent to 1.

| Rxn ID | Reaction                                 | $A$<br>$\text{cm}^3 \text{ molec}^{-1} \text{ s}^{-1}$ | $E_a/R$<br>K | Citation                      |
|--------|--|--|--------------|-------------------------------|
| M1     | $I + O_3 \rightarrow IO + O_2$           | $2.10 \times 10^{-11}$                                 | -830         | Atkinson et al. (2007)        |
| M2     | $I + HO_2 \rightarrow HI + O_2$          | $1.50 \times 10^{-11}$                                 | -1090        | Sander et al. (2011)          |
| M3     | $I_2 + OH \rightarrow HOI + I$           | $2.10 \times 10^{-10}$                                 | -            | Atkinson et al. (2007)        |
| M4     | $HI + OH \rightarrow I + H_2O$           | $1.60 \times 10^{-11}$                                 | 440          | Atkinson et al. (2007)        |
| M5     | $HOI + OH \rightarrow IO + H_2O$         | $5.00 \times 10^{-12}$                                 | -            | Riffault et al. (2005)        |
| M6     | $IO + HO_2 \rightarrow HOI + O_2$        | $1.40 \times 10^{-11}$                                 | 540          | Atkinson et al. (2007)        |
| M7     | $IO + NO \rightarrow I + NO_2$           | $7.15 \times 10^{-12}$                                 | 300          | Atkinson et al. (2007)        |
| M8     | $HO + CH_3I \rightarrow H_2O + I(CH_2I)$ | $4.30 \times 10^{-12}$                                 | -1120        | Atkinson et al. (2008)        |
| M9     | $INO + INO \rightarrow I_2 + 2NO$        | $8.40 \times 10^{-11}$                                 | -2620        | Atkinson et al. (2007)        |
| M10    | $INO_2 + INO_2 \rightarrow I_2 + 2NO_2$  | $4.70 \times 10^{-12}$                                 | -1670        | Atkinson et al. (2007)        |
| M11    | $I_2 + NO_3 \rightarrow I + INO_3$       | $1.50 \times 10^{-12}$                                 | -            | Atkinson et al. (2007)        |
| M12    | $INO_3 + I \rightarrow I_2 + NO_3$       | $9.10 \times 10^{-11}$                                 | -146         | Kaltsoyannis and Plane (2008) |
| M13    | $I + BrO \rightarrow IO + Br$            | $1.20 \times 10^{-11}$                                 | -            | Sander et al. (2011)          |
| M14    | $IO + Br \rightarrow I + BrO$            | $2.70 \times 10^{-11}$                                 | -            | Bedjanian et al. (1997)       |
| M15    | $IO + BrO \rightarrow Br + I + O_2$      | $3.00 \times 10^{-12}$                                 | 510          | Atkinson et al. (2007)        |
| M16    | $IO + BrO \rightarrow Br + OIO$          | $1.20 \times 10^{-11}$                                 | 510          | Atkinson et al. (2007)        |
| M17    | $OIO + OIO \rightarrow I_2O_4$           | $1.50 \times 10^{-10}$                                 | -            | Gómez Martín et al. (2007)    |
| M18    | $OIO + NO \rightarrow NO_2 + IO$         | $1.10 \times 10^{-12}$                                 | 542          | Atkinson et al. (2007)        |

## Iodine's impact on tropospheric oxidants: a global model study in GEOS-Chem

T. Sherwen et al.

[Title Page](#)

[Abstract](#)

[Introduction](#)

[Conclusions](#)

[References](#)

[Tables](#)

[Figures](#)

[|◀](#)

[▶|](#)

[Back](#)

[Close](#)

[Full Screen / Esc](#)

[Printer-friendly Version](#)

[Interactive Discussion](#)

## Iodine's impact on tropospheric oxidants: a global model study in GEOS-Chem

T. Sherwen et al.

**Table 4.** Termolecular iodine reactions. The lower pressure limit rate ( $k_0$ ) is given by:  $A_0 \cdot \exp(\frac{Ea_0}{RT}) \cdot (\frac{300}{T})^x$ . The high pressure limit rate  $k(\infty)$  is given by:  $A_\infty \cdot \exp(\frac{Ea_\infty}{RT})$ . Fc characterises the fall off curve of the reaction as described by Atkinson et al. (2007). Unknown values are represented by a dash and these set to zero in the model, reducing the exponent to 1. Reverse equilibrium reaction rates ( $K_{eq}$ ) for T3\* and T5\* are from Atkinson et al. (2007) given as  $1.0 \times 10^{-6} \exp(9160/T)$  and  $1.0 \times 10^{-6} \exp(9200/T)$  respectively.

| Rxn ID | Reaction   | $A_0$<br>cm <sup>3</sup> molec <sup>-1</sup> s <sup>-1</sup> | $Ea_0/R$<br>K | x | $A_\infty$<br>cm <sup>3</sup> molec <sup>-1</sup> s <sup>-1</sup> | $Ea_\infty/R$<br>K | Fc   | Citation                      |
|--------|--|--|---------------|---|---|--------------------|------|-------------------------------|
| T1     | $\text{IO} + \text{IO} + \text{O}_2 \rightarrow \text{I} + \text{OIO}$ | $2.16 \times 10^{-11}$                                       | 180           | — | —   | —                  | —    | Atkinson et al. (2007)        |
| T2     | $\text{IO} + \text{IO} + \text{O}_2 \rightarrow \text{I}_2\text{O}_2$  | $3.24 \times 10^{-11}$                                       | 180           | — | —   | —                  | —    | Atkinson et al. (2007)        |
| T3*    | $\text{I} + \text{NO} + \text{M} \rightleftharpoons \text{INO}$        | $1.80 \times 10^{-32}$                                       | 300           | 1 | $1.70 \times 10^{-11}$  | 9200               | 0.60 | Atkinson et al. (2007)        |
| T4     | $\text{INO} \rightarrow \text{I} + \text{NO}$                          | $2.00 \times 10^{-5}$  | —             | — | —   | —                  | —    | Atkinson et al. (2007)        |
| T5*    | $\text{I} + \text{NO}_2 + \text{M} \rightleftharpoons \text{INO}_2$    | $3.00 \times 10^{-31}$                                       | 300           | 1 | $6.60 \times 10^{-11}$  | 96000              | 0.63 | Atkinson et al. (2007)        |
| T6     | $\text{INO}_2 \rightarrow \text{I} + \text{NO}_2$                      | $3.72 \times 10^{-7}$  | —             | — | —   | —                  | —    | Atkinson et al. (2007)        |
| T7     | $\text{IO} + \text{NO}_2 \rightarrow \text{INO}_3$                     | $7.70 \times 10^{-31}$                                       | —             | 5 | $1.60 \times 10^{-11}$  | —                  | 0.40 | Atkinson et al. (2007)        |
| T8     | $\text{INO}_3 + \text{M} \rightarrow \text{IO} + \text{NO}_2$          | $2.10 \times 10^{15}$  | -13670        | — | —   | —                  | 0.60 | Kaltsoyannis and Plane (2008) |
| T9     | $\text{IO} + \text{OIO} + \text{M} \rightarrow \text{I}_2\text{O}_3$   | $1.50 \times 10^{-10}$                                       | —             | — | —   | —                  | —    | Gómez Martín et al. (2007)    |
| T10    | $\text{I}_2\text{O}_2 + \text{M} \rightarrow \text{IO} + \text{IO}$    | $1.00 \times 10^{12}$  | -9770         | — | —   | —                  | 0.60 | Ordóñez et al. (2012)         |
| T11    | $\text{I}_2\text{O}_2 + \text{M} \rightarrow \text{OIO} + \text{I}$    | $2.50 \times 10^{14}$  | -9770         | — | —   | —                  | 0.60 | Ordóñez et al. (2012)         |
| T12    | $\text{I}_2\text{O}_4 + \text{M} \rightarrow 2\text{OIO}$              | $3.80 \times 10^{-2}$  | —             | — | —   | —                  | —    | Kaltsoyannis and Plane (2008) |

| Title Page               |              |
|--------------------------|--------------|
| Abstract                 | Introduction |
| Conclusions              | References   |
| Tables                   | Figures      |
|                          |              |
|                          |              |
| Back                     | Close        |
| Full Screen / Esc        |              |
| Printer-friendly Version |              |
| Interactive Discussion   |              |

## Iodine's impact on tropospheric oxidants: a global model study in GEOS-Chem

T. Sherwen et al.

[Title Page](#)

[Abstract](#)

[Introduction](#)

[Conclusions](#)

[References](#)

[Tables](#)

[Figures](#)

[|◀](#)

[▶|](#)

[◀](#)

[▶](#)

[Back](#)

[Close](#)

[Full Screen / Esc](#)

[Printer-friendly Version](#)

[Interactive Discussion](#)



**Table 5.** Photolysis reactions of iodine species. For  $I_2O_X$  ( $X = 2, 3, 4$ ) the cross-section of  $INO_3$  is used as described in Sect. 2.4.

| ID  | Reaction                                  | Reference cross-section |
|-----|---|-------------------------|
| J1  | $I_2 + h\nu \rightarrow 2I$               | Sander et al. (2011)    |
| J2  | $HOI + h\nu \rightarrow I + OH$           | Sander et al. (2011)    |
| J3  | $IO + h\nu \rightarrow I + [O_3]$         | Sander et al. (2011)    |
| J4  | $OIO + h\nu \rightarrow I + O_2$          | Sander et al. (2011)    |
| J5  | $INO + h\nu \rightarrow I + NO$           | Sander et al. (2011)    |
| J6  | $INO_2 + h\nu \rightarrow I + NO_2$       | Sander et al. (2011)    |
| J7  | $INO_3 + h\nu \rightarrow I + NO_3$       | Sander et al. (2011)    |
| J8  | $I_2O_2 + h\nu \rightarrow I + OIO$       | see Sect. 2.4           |
| J9  | $CH_3I + h\nu \rightarrow I + CH_2O_2$    | Sander et al. (2011)    |
| J10 | $CH_2I_2 + h\nu \rightarrow 2I + (CH_2)$  | Sander et al. (2011)    |
| J11 | $CH_2ICl + h\nu \rightarrow I + (CH_2Cl)$ | Sander et al. (2011)    |
| J12 | $CH_2IBr + h\nu \rightarrow I + (CH_2Br)$ | Sander et al. (2011)    |
| J20 | $I_2O_4 + h\nu \rightarrow 2OIO$          | see Sect. 2.4           |
| J21 | $I_2O_3 + h\nu \rightarrow OIO + IO$      | see Sect. 2.4.          |

## Iodine's impact on tropospheric oxidants: a global model study in GEOS-Chem

T. Sherwen et al.

**Table 6.** Heterogeneous reactions of iodine species. Where measured values have not been reported estimated values are used and no reference is given, further detail on uptake choices is in Sect. A1.2. Stared (\*) reactions proceed only on sea-salt aerosols.

| ID | Reaction   | Reactive uptake coefficient ( $\gamma$ ) | Reference             |
|----|--|--|-----------------------|
| K1 | $\text{HI} \rightarrow \text{iodine aerosol}$            | 0.10*                                    | Crowley et al. (2010) |
| K2 | $\text{INO}_3 \rightarrow 0.5\text{I}_2$                 | 0.01*                                    | see caption text      |
| K3 | $\text{HOI} \rightarrow 0.5\text{I}_2$                   | 0.01*                                    | Sander et al. (2011)  |
| K4 | $\text{INO}_2 \rightarrow 0.5\text{I}_2$                 | 0.02*                                    | see caption text      |
| K5 | $\text{I}_2\text{O}_2 \rightarrow \text{iodine aerosol}$ | 0.02                                     | see caption text      |
| K6 | $\text{I}_2\text{O}_4 \rightarrow \text{iodine aerosol}$ | 0.02                                     | see caption text      |
| K7 | $\text{I}_2\text{O}_3 \rightarrow \text{iodine aerosol}$ | 0.02                                     | see caption text      |

**Table 7.** Comparison between global tropospheric O<sub>X</sub> budgets of standard GEOS-Chem (v9-2) which includes bromine chemistry and the iodine simulation described here which includes both iodine and bromine chemistry. Recent average model values from Young et al. (2013) are also shown. For the IO+BrO halogen crossover reaction we allocate half the O<sub>3</sub> loss to bromine and half to iodine. Values are rounded to the nearest integer value.

| Scenario  | GEOS-Chem simulation (v9-2) | Iodine simulation | ACCENT Young et al. (2013) |
|---|-----------------------------|-------------------|----------------------------|
| O <sub>3</sub> burden (Tg)  | 367                         | 334               | 340 ± 40                   |
| O <sub>x</sub> chemical Sources (Tg Yr <sup>-1</sup> )                                |                             |                   |                            |
| NO + HO <sub>2</sub>  | 3512                        | 3529              | —                          |
| NO + CH <sub>3</sub> O <sub>2</sub>   | 1269                        | 1307              | —                          |
| Other O <sub>x</sub> sources  | 505                         | 521               | —                          |
| Total chemical O <sub>x</sub> sources (PO <sub>x</sub> )                              | 5286                        | 5357              | 5110 ± 606                 |
| O <sub>x</sub> chemical sinks (Tg Yr <sup>-1</sup> )                                  |                             |                   |                            |
| O <sub>3</sub> + hν + H <sub>2</sub> O → 2OH  | 2425                        | 2119              | —                          |
| O <sub>3</sub> + HO <sub>2</sub> → OH + O <sub>2</sub>                                | 1274                        | 1080              | —                          |
| O <sub>3</sub> + OH → HO <sub>2</sub> + O <sub>2</sub>                                | 621                         | 560               | —                          |
| HOBr + hν → Br + OH   | 166                         | 143               | —                          |
| HOBr + HBr → Br <sub>2</sub> + H <sub>2</sub> O (aq. aerosol)                         | 8                           | 8                 | —                          |
| BrO + BrO → 2Br + O <sub>2</sub>  | 12                          | 10                | —                          |
| BrO + BrO → Br <sub>2</sub> + O <sub>2</sub>  | 3                           | 3                 | —                          |
| BrO + OH → Br + HO <sub>2</sub>   | 6                           | 5                 | —                          |
| IO + BrO → Br + I + O <sub>2</sub>  | —                           | 7                 | —                          |
| Other bromine O <sub>x</sub> sinks  | 1                           | 1                 | —                          |
| Total bromine O <sub>x</sub> sinks  | 195                         | 178               | —                          |
| HOI + hν → I + OH   | —                           | 583               | —                          |
| HOI → 0.5I <sub>2</sub> (seasalt aerosol)   | —                           | 2                 | —                          |
| IO + BrO → Br + I + O <sub>2</sub>  | —                           | 7                 | —                          |
| OIO + hν → I + O <sub>2</sub>   | —                           | 156               | —                          |
| Other iodine O <sub>x</sub> sinks   | —                           | 1                 | —                          |
| Total iodine O <sub>x</sub> sinks   | —                           | 748               | —                          |
| Other O <sub>x</sub> sinks  | 172                         | 173               | —                          |
| Total chem. O <sub>x</sub> sinks (LO <sub>x</sub> )                                   | 4687                        | 4864              | 4668 ± 727                 |
| O <sub>3</sub> P(O <sub>x</sub> )-L(O <sub>x</sub> ) (Tg Yr <sup>-1</sup> )           | 599                         | 493               | 442 (aprox.)               |
| O <sub>3</sub> Dry deposition (Tg Yr <sup>-1</sup> )                                  | 886                         | 791               | 1003 ± 200                 |
| O <sub>3</sub> Lifetime (days)  | 24                          | 22                | 22 ± 2                     |
| O <sub>3</sub> STE (PO <sub>x</sub> -LO <sub>x</sub> Dry dep.) (Tg Yr <sup>-1</sup> ) | 287                         | 298               | 552 ± 168                  |

# Iodine's impact on tropospheric oxidants: a global model study in GEOS-Chem

T. Sherwen et al.

Title Page

## Abstract

Introduction

## Conclusions

## References

## Tables

## Figures

Back

Close

Full Screen / Esc

[Printer-friendly Version](#)

## Interactive Discussion



## Iodine's impact on tropospheric oxidants: a global model study in GEOS-Chem

T. Sherwen et al.

**Table A1.** Effects of sensitivity runs on relevant variables. Values are shown as percentage change from the iodine simulation in the troposphere as global means unless otherwise stated. MBL = Marine Boundary Layer ( $900 < hPa$ ),  $O_X$  is defined as in the text.  $CH_4$  lifetime is calculated globally in the troposphere with respect to loss by reaction with OH.

|                                       | Mean IO MBL surface concentration | Chem. $O_X$ loss ( $LO_X$ ) | Chem. $O_X$ prod. ( $PO_X$ ) | $PO_X$ - $LO_X$ | $O_3$ burden | $O_3$ deposition |
|---------------------------------------|-----------------------------------|-----------------------------|------------------------------|-----------------|--------------|------------------|
| Just org. I                           | -83.45                            | -1.64                       | -3.11                        | 17.69           | 5.53         | 7.19             |
| $I_2O_X$ loss ( $\gamma$ ) $\times 2$ | -4.26                             | -0.15                       | -0.28                        | 1.61            | 0.54         | 0.59             |
| $I_2O_X$ loss ( $\gamma$ )/2          | 3.93                              | 0.13                        | 0.24                         | -1.34           | -0.44        | -0.52            |
| Het. cycle ( $\gamma$ ) $\times 2$    | 2.21                              | 0.04                        | 0.16                         | -1.61           | -0.69        | -0.56            |
| Het. cycle ( $\gamma$ )/2             | -1.84                             | -0.06                       | -0.14                        | 1.07            | 0.56         | 0.45             |
| No Het. cycle                         | -48.03                            | -1.15                       | -2.20                        | 12.60           | 4.09         | 5.23             |
| Sulphate Uptake                       | -22.49                            | -1.25                       | -2.26                        | 12.06           | 4.54         | 4.94             |
| Ocean iodide                          | -34.28                            | -0.66                       | -1.26                        | 7.24            | 2.06         | 3.01             |
| $I_2O_X$ X-sections $\times 2$        | 4.30                              | 0.11                        | 0.22                         | -1.34           | -0.40        | -0.47            |
| $I_2O_X$ exp. X-sections              | 6.73                              | 0.19                        | 0.35                         | -1.88           | -0.60        | -0.73            |
| No $I_2O_X$ Photolysis                | -39.35                            | -1.10                       | -2.12                        | 12.33           | 5.05         | 4.86             |
| MBL BrO 2 pptv                        | -6.78                             | -3.59                       | -2.71                        | -15.28          | -3.73        | -6.03            |

|  |                            |                              |
|--|----------------------------|------------------------------|
| <a href="#">Title Page</a>               | <a href="#">Abstract</a>   | <a href="#">Introduction</a> |
| <a href="#">Conclusions</a>              | <a href="#">References</a> |                              |
| <a href="#">Tables</a>                   | <a href="#">Figures</a>    |                              |
| <a href="#">◀</a>                        | <a href="#">▶</a>          |                              |
| <a href="#">◀</a>                        | <a href="#">▶</a>          |                              |
| <a href="#">Back</a>                     | <a href="#">Close</a>      |                              |
| <a href="#">Full Screen / Esc</a>        |                            |                              |
| <a href="#">Printer-friendly Version</a> |                            |                              |
| <a href="#">Interactive Discussion</a>   |                            |                              |

## Iodine's impact on tropospheric oxidants: a global model study in GEOS-Chem

T. Sherwen et al.

[Title Page](#)

[Abstract](#)

[Introduction](#)

[Conclusions](#)

[References](#)

[Tables](#)

[Figures](#)

[|◀](#)

[▶|](#)

[◀](#)

[▶](#)

[Back](#)

[Close](#)

[Full Screen / Esc](#)

[Printer-friendly Version](#)

[Interactive Discussion](#)

**Table A1.** Continued.

|  | OH mean concentration | HO <sub>2</sub> mean concentration | HO <sub>2</sub> /OH | I <sub>Y</sub> lifetime | IO <sub>X</sub> lifetime | I <sub>Y</sub> burden | CH <sub>4</sub> lifetime |
|--|-----------------------|------------------------------------|---------------------|-------------------------|--------------------------|-----------------------|--------------------------|
| Just org. I  | -0.64                 | 3.53                               | 4.19                | 123.92                  | 16.09                    | -64.26                | 0.21                     |
| I <sub>2</sub> O <sub>X</sub> loss ( $\gamma$ ) ×2 | -0.08                 | 0.27                               | 0.36                | -8.38                   | -0.93                    | -5.08                 | 0.03                     |
| I <sub>2</sub> O <sub>X</sub> loss ( $\gamma$ ) /2 | 0.05                  | -0.22                              | -0.27               | 8.00                    | 0.55                     | 4.27                  | -0.01                    |
| Het. cycle ( $\gamma$ ) ×2                         | 0.09                  | -0.39                              | -0.49               | 4.61                    | 1.13                     | 5.98                  | 0.00                     |
| Het. cycle ( $\gamma$ ) /2                         | -0.09                 | 0.32                               | 0.41                | -3.89                   | -0.96                    | -5.04                 | 0.02                     |
| No Het. cycle                                      | -0.47                 | 2.58                               | 3.07                | -61.18                  | 5.38                     | -46.69                | 0.15                     |
| Sulphate Uptake                                    | -0.87                 | 2.70                               | 3.60                | -59.60                  | 0.49                     | -48.49                | 0.52                     |
| Ocean iodide                                       | -0.17                 | 1.22                               | 1.39                | 16.90                   | 2.77                     | -23.42                | 0.01                     |
| I <sub>2</sub> O <sub>X</sub> X-sections ×2        | 0.05                  | -0.20                              | -0.25               | 5.26                    | 0.61                     | 3.10                  | -0.01                    |
| I <sub>2</sub> O <sub>X</sub> exp. X-sections      | 0.08                  | -0.31                              | -0.39               | 8.31                    | 0.84                     | 4.81                  | -0.01                    |
| No I <sub>2</sub> O <sub>X</sub> Photolysis        | -0.90                 | 2.54                               | 3.48                | -46.41                  | -17.68                   | -34.58                | 0.32                     |
| MBL BrO 2 pptv                                     | -3.31                 | -1.44                              | 1.93                | -3.72                   | 3.33                     | -10.07                | 4.17                     |

## Iodine's impact on tropospheric oxidants: a global model study in GEOS-Chem

T. Sherwen et al.

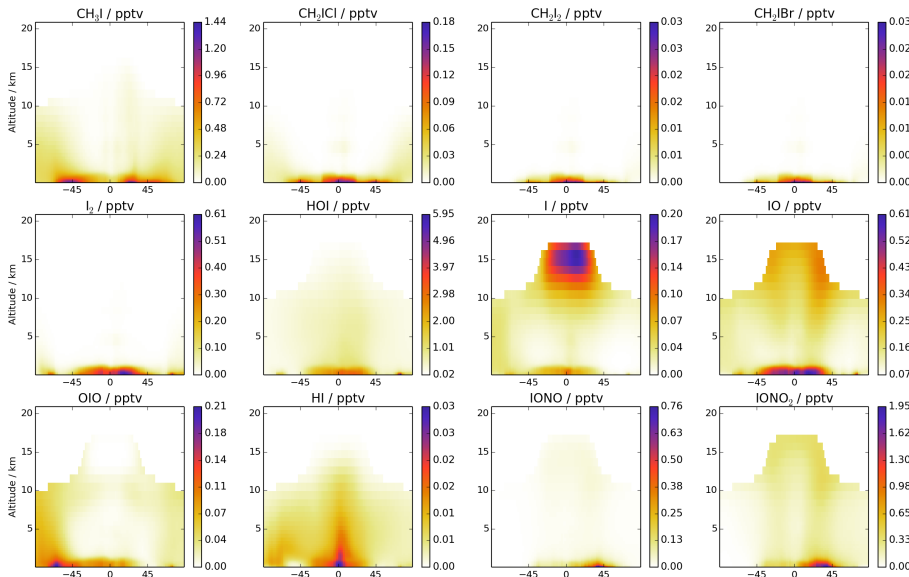


**Figure 1.** Annual mean zonal tropospheric mixing ratios for precursor and reactive iodine compounds (pptv). No calculations of concentrations are made within the stratosphere and so that region is left blank.

- [Title Page](#)
- [Abstract](#) [Introduction](#)
- [Conclusions](#) [References](#)
- [Tables](#) [Figures](#)
- [◀](#) [▶](#)
- [◀](#) [▶](#)
- [Back](#) [Close](#)
- [Full Screen / Esc](#)
- [Printer-friendly Version](#)
- [Interactive Discussion](#)

## Iodine's impact on tropospheric oxidants: a global model study in GEOS-Chem

T. Sherwen et al.

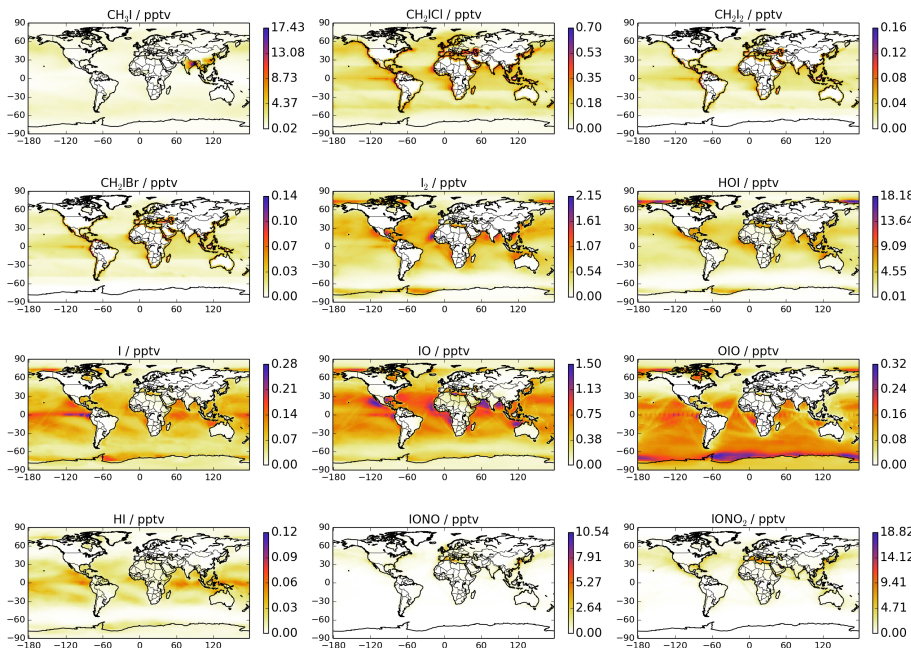


**Figure 2.** Annual mean surface mixing ratios for precursor and reactive iodine (pptv).

**Iodine's impact on tropospheric oxidants: a global model study in GEOS-Chem**

T. Sherwen et al.

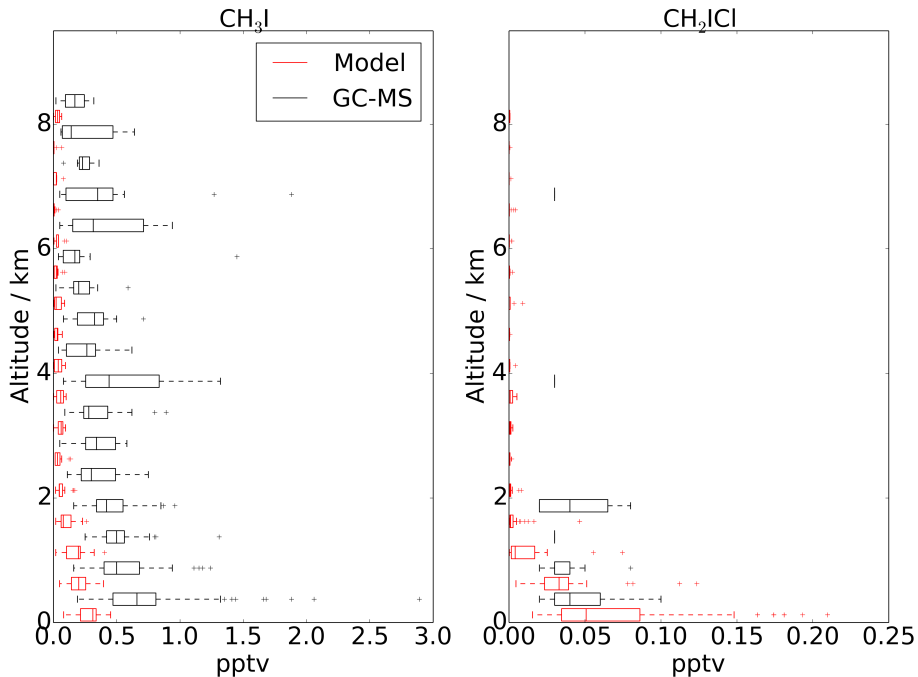


**Figure 3.** Vertical comparison of observations from the CAST (Combined Airborne Studies in the Tropics) campaign in the mid Pacific (Guam). The observations are shown in black and modelled values in red. The observations are from the FAAM BAE-146 research aircraft Whole Air Samples (WAS) analysed by Gas Chromatography-Mass Spectrometry (GC-MS). The box-plot extents give the inter-quartile range, with the median shown within the box. The whiskers give the most extreme point within 1.5 times the inter-quartile range.

## Iodine's impact on tropospheric oxidants: a global model study in GEOS-Chem

T. Sherwen et al.

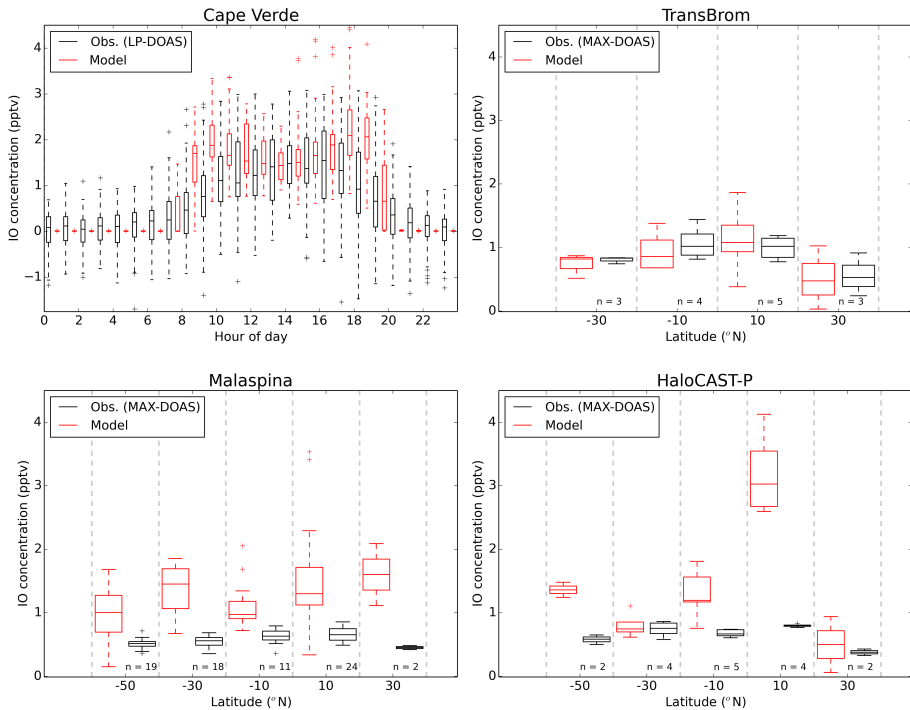


**Figure 4.** Iodine oxide (IO) surface observations (red) by campaign compared against model (black). Cape Verde measurements are shown against hour of day and others are shown as a function of latitude. Observations are from Cape Verde (Tropical Atlantic Mahajan et al., 2010; Read et al., 2008), Transbrom (West Pacific, Großmann et al., 2013), the Malaspina circumnavigation (Prados-Roman et al., 2015b), and HaloCAST-P (East Pacific, Mahajan et al., 2012). Number of data points within latitudinal bin are shown as “n”. The boxplot extents give the inter-quartile range, with the median shown within the box. The whiskers give the most extreme point within 1.5 times the inter-quartile range.

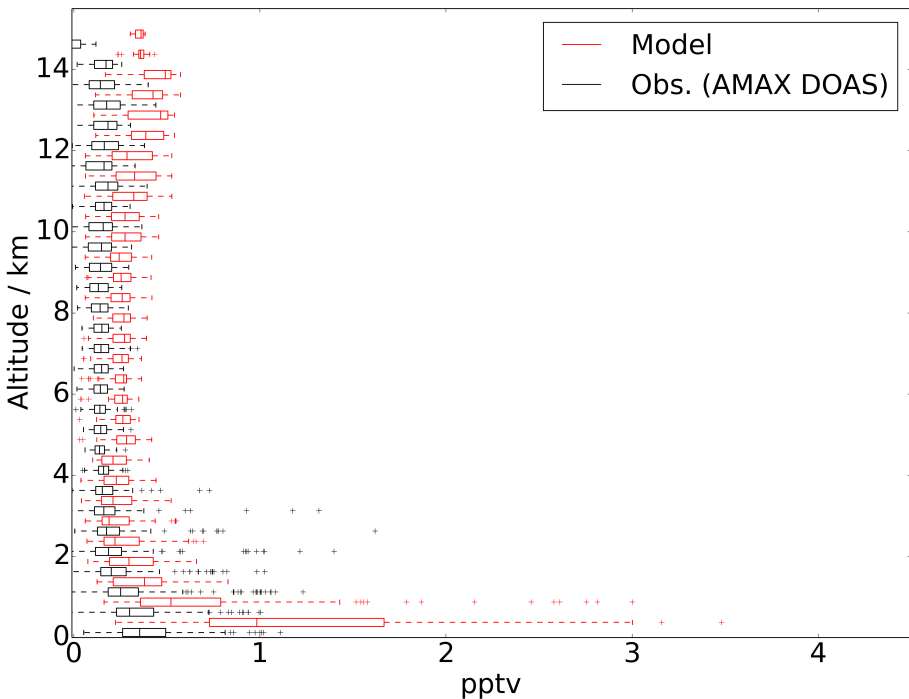


**Figure 5.** Vertical comparison of modelled and measured iodine oxide (IO) during the TORERO research campaign. Model and observations are in red and black respectively. Measurements were taken aboard the NSF/NCAR GV research aircraft by the University of Colorado airborne Multi-Axis DOAS instrument (CU AMAX-DOAS) as part of the TORERO campaign (Volkamer et al., 2015; Wang et al., 2015) in the eastern Pacific in January and February 2012. The boxplot extents give the inter-quartile range, with the median shown within the box. The whiskers give the most extreme point within 1.5 times the inter-quartile range.

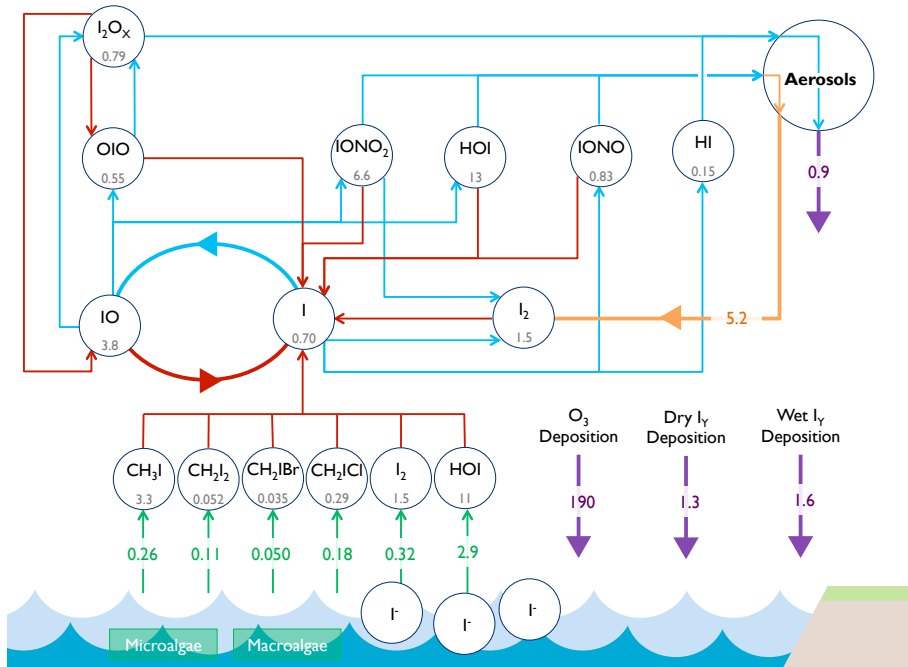


**Figure 6.** Schematic representation of implemented iodine chemistry. Average global annual mean burdens (Gg I) are shown below key  $I_Y$  species, with fluxes ( $Tg\text{I yr}^{-1}$ ) shown on arrows. Red lines = photolysis, blue = chemical pathways, green lines = emission source, orange lines = heterogeneous pathway. This equates to a total iodine source and sink of  $3.8\text{Tg}\text{I yr}^{-1}$ .  $O_3$  deposition in Tg is also shown to illustrate the driving force behind the inorganic emissions.

# Iodine's impact on tropospheric oxidants: a global model study in GEOS-Chem

T. Sherwen et al.

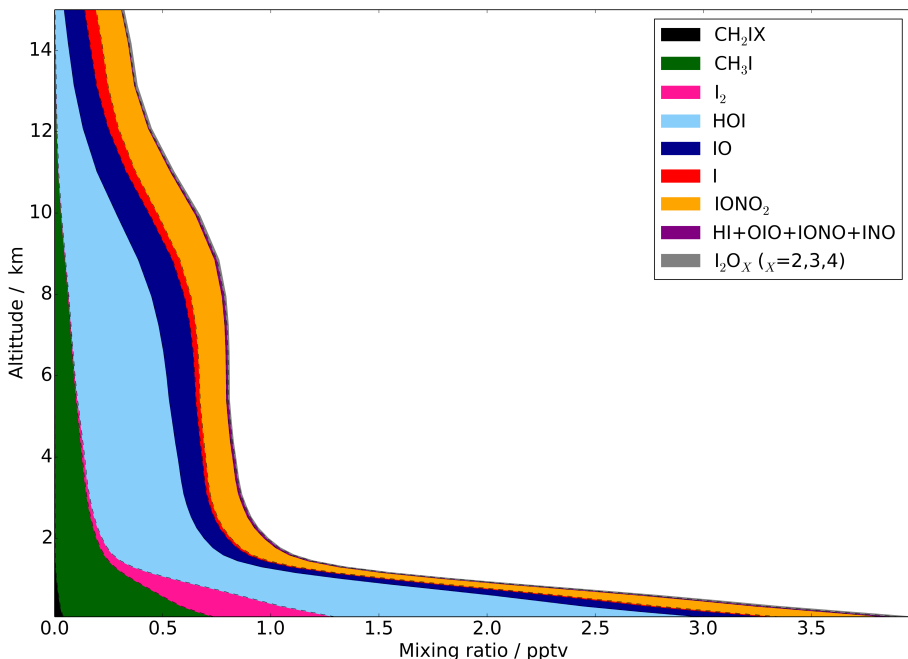


**Figure 7.** Global annual mean gas-phase iodine speciation with altitude. Mixing ratios are shown in pptv, with higher iodine oxides ( $I_2O_X$  ( $X = 2, 3, 4$ )) and di-halogenated organics ( $CH_2IX$  ( $X = Cl, Br, I$ )) grouped.

Title Page

## Abstract

Introduction

## Conclusio

## References

## Tables

Figures

1

1

Back

[Close](#)

Full Screen / Esc

Interactive Discussion

## Iodine's impact on tropospheric oxidants: a global model study in GEOS-Chem

T. Sherwen et al.

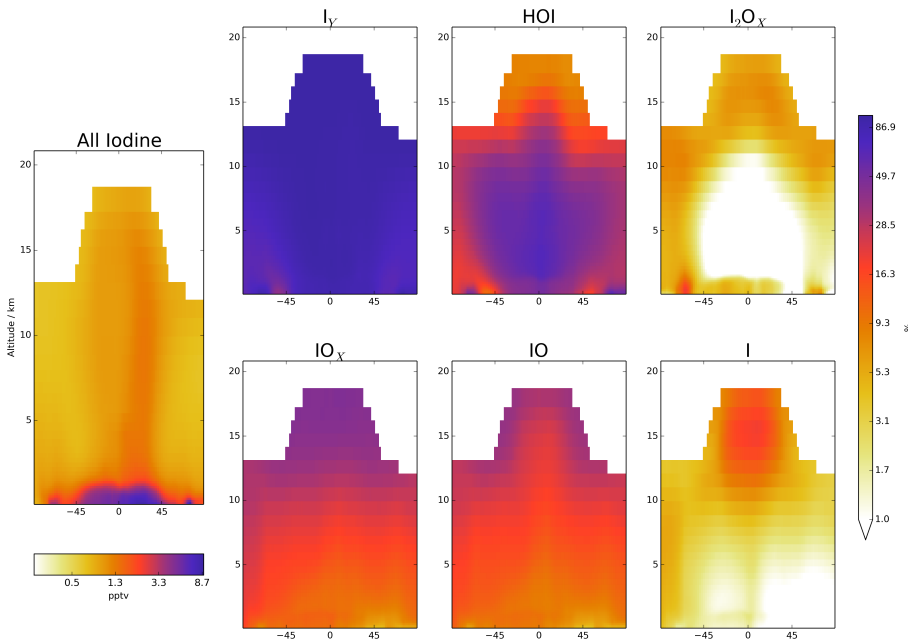


**Figure 8.** Zonal breakdown of global annual mean iodine speciation by family. First panel shows total gas phase iodine concentration and the following panels show percentage of different compounds to this. Total gas phase iodine =  $\text{CH}_3\text{I} + 2\text{CH}_2\text{I}_2 + \text{CH}_2\text{IBr} + \text{CH}_2\text{ICl} + 2\text{I}_2 + \text{HOI} + \text{IO} + \text{OIO} + \text{HI} + \text{INO}_2 + \text{INO}_3 + 2\text{I}_2\text{O}_2 + 2\text{I}_2\text{O}_3 + 2\text{I}_2\text{O}_4 + \text{I} + \text{INO}$ ;  $\text{I}_Y = 2\text{I}_2 + \text{HOI} + \text{IO} + \text{OIO} + \text{HI} + \text{INO}_2 + \text{INO}_3 + 2\text{I}_2\text{O}_2 + 2\text{I}_2\text{O}_3 + 2\text{I}_2\text{O}_4$ ;  $\text{IO}_X = \text{I} + \text{IO}$ .

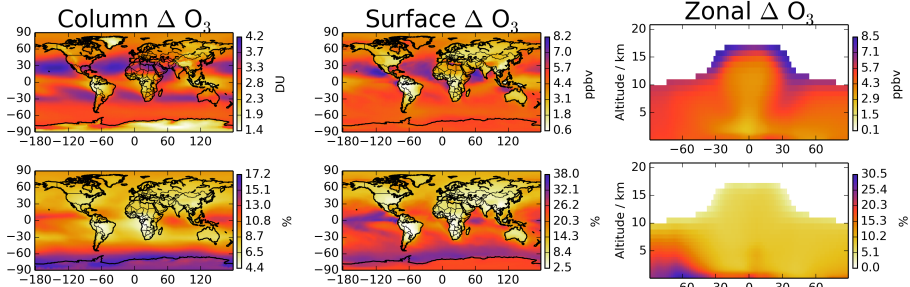


**Figure 9.** Decreases in annual mean tropospheric column, surface and zonal  $O_3$  with inclusion of iodine chemistry are shown on left, middle and right panels respectively. Upper panels show changes in Dobson units or ppbv and lower panels show changes in percentage terms. This is calculated as the difference in the  $O_3$  concentrations between standard GEOS-Chem (v9-2, including bromine) and the iodine simulation.

Title Page

## Abstract

## Introduction

## Conclusions

## References

Tables

## Figures

Back

Close

Full Screen / Esc

Interactive Discussion

## Iodine's impact on tropospheric oxidants: a global model study in GEOS-Chem

T. Sherwen et al.

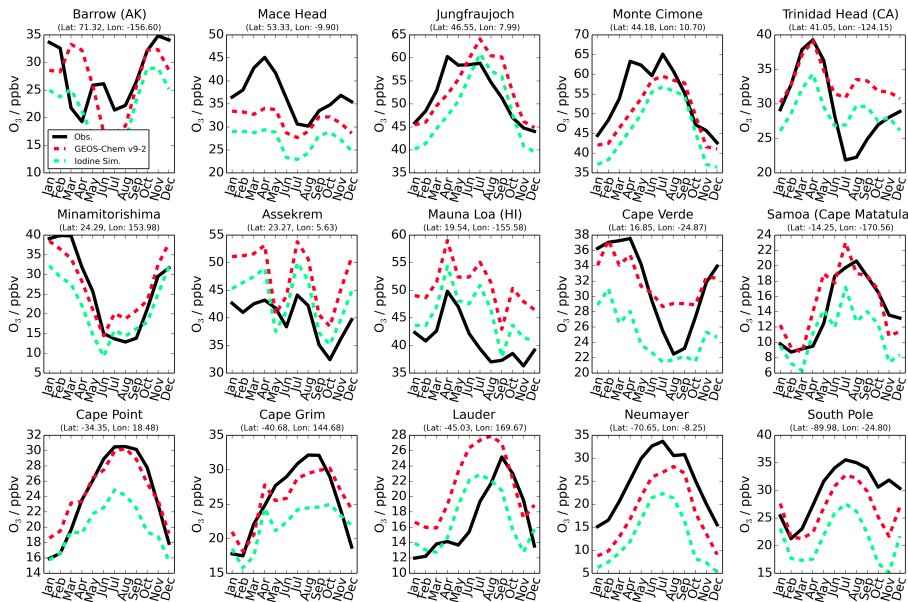


**Figure 10.** Seasonal cycle of near-surface O<sub>3</sub> at a range of Global Atmospheric Watch (GAW) sites (Sofen et al., 2015). Observational data shown is a 6 year monthly average (2006–2012). Model data is for 2005. Data is from GAW compile and processed as described in (Sofen et al., 2015). Red indicates standard GEOS-Chem (v9-2, including bromine) and green with inclusion of iodine chemistry.

- [Title Page](#)
- [Abstract](#) [Introduction](#)
- [Conclusions](#) [References](#)
- [Tables](#) [Figures](#)
- [◀](#) [▶](#)
- [◀](#) [▶](#)
- [Back](#) [Close](#)
- [Full Screen / Esc](#)
- [Printer-friendly Version](#)
- [Interactive Discussion](#)

## Iodine's impact on tropospheric oxidants: a global model study in GEOS-Chem

T. Sherwen et al.

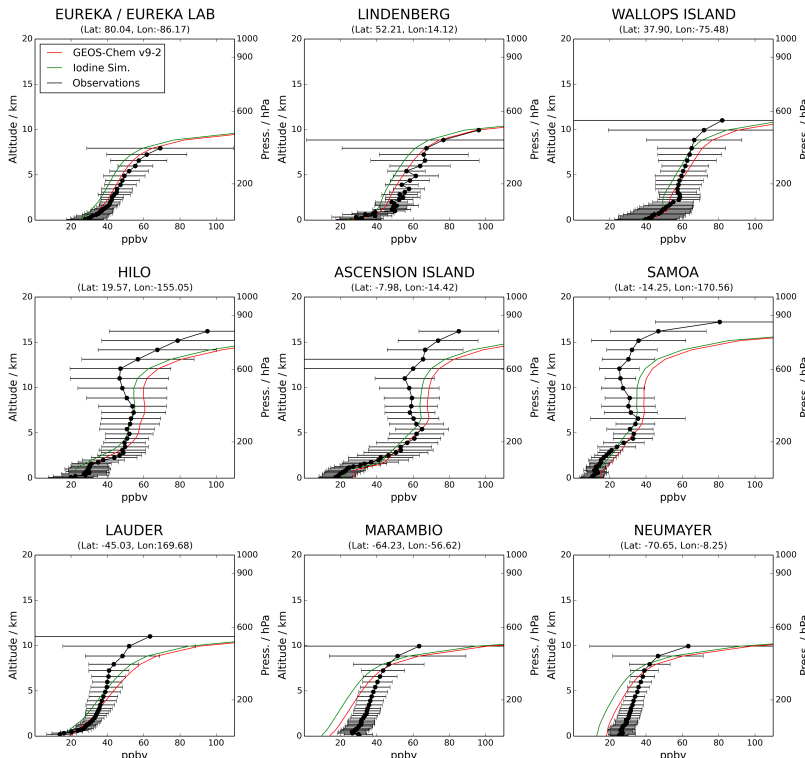


**Figure 11.** Comparison between annual modelled O<sub>3</sub> profiles and sonde data (2005, WOUDC, 2014). Profiles shown are the annual mean of available observations from World Ozone and Ultraviolet Radiation Data Centre WOUDC (2014) and model data for 2005 at given locations. The standard GEOS-Chem (v9-2) and the iodine simulation are shown in red and green respectively. Observations (in black) show mean concentrations with upper and lower quartiles given by whiskers.

# Iodine's impact on tropospheric oxidants: a global model study in GEOS-Chem

T. Sherwen et al.

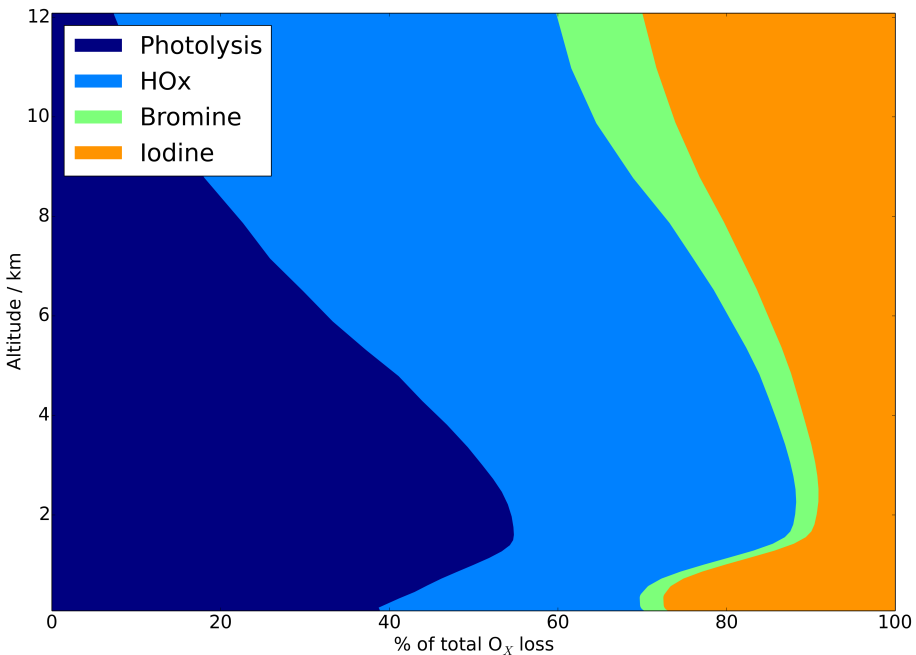


**Figure 12.** Vertical profile of simulated fractional global annual mean  $O_X$  loss by route.  $O_X$  definition is given in text. Photolysis represents loss of  $O_X$  due to  $O_3$  photolysis in the presence of water vapour.  $HO_X$  loss includes routes via minor  $NO_X$  channels. The magnitude of the bromine route is probably underestimated as discussed in Sect. 2.6.

21019

| Title Page               |              |
|--------------------------|--------------|
| Abstract                 | Introduction |
| Conclusions              | References   |
| Tables                   | Figures      |
| ◀                        | ▶            |
| ◀                        | ▶            |
| Back                     | Close        |
| Full Screen / Esc        |              |
| Printer-friendly Version |              |
| Interactive Discussion   |              |



**Iodine's impact on tropospheric oxidants: a global model study in GEOS-Chem**

T. Sherwen et al.

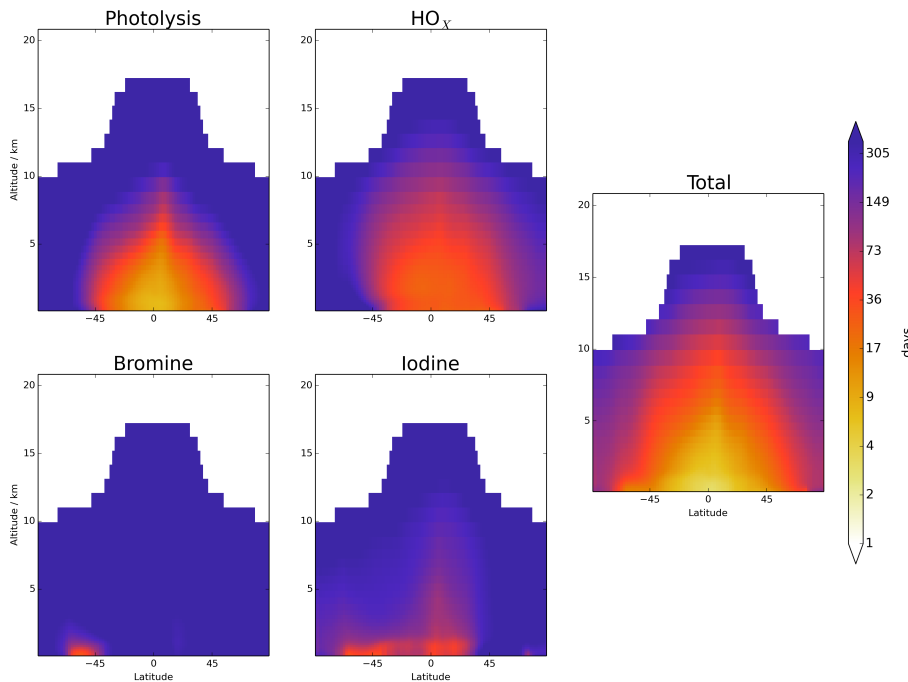


**Figure 13.** Global annual  $\text{O}_3$  mean zonal chemical lifetime for different  $\text{O}_X$  loss routes (Photolysis,  $\text{HO}_X$ , Iodine, Bromine, and Total). Values are shown on a log on a scale.

# Iodine's impact on tropospheric oxidants: a global model study in GEOS-Chem

T. Sherwen et al.

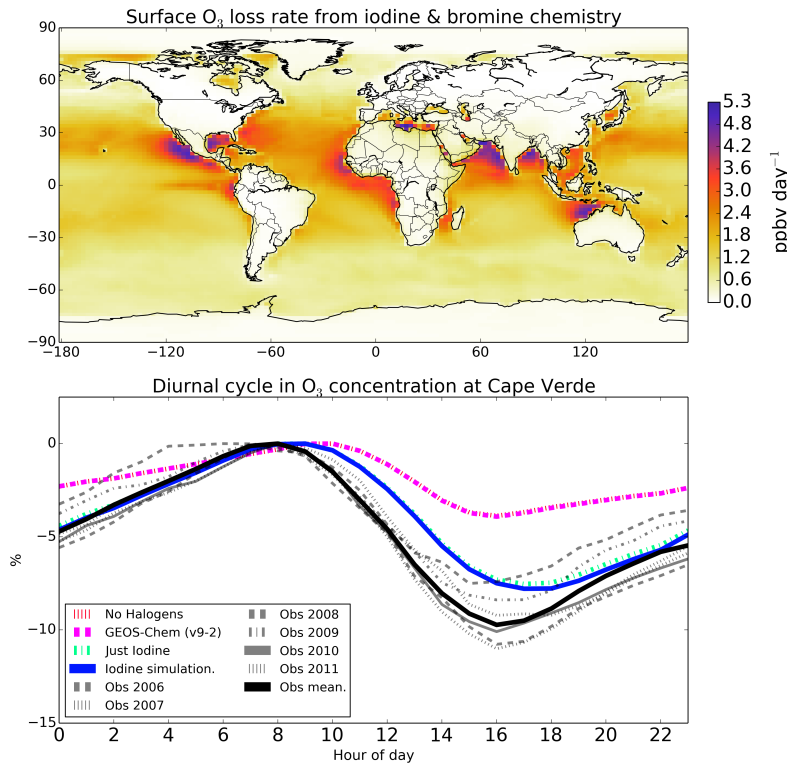


**Figure 14.** Global annual mean surface O<sub>3</sub> loss (ppbv day<sup>-1</sup>) from both bromine and iodine compared to a simulation with neither (top), comparison between modelled and observed fractional diurnal O<sub>3</sub> cycles at the Cape Verde Observatory for 4 simulations (bottom). The diurnal change is calculated by subtracting each day's maximum O<sub>3</sub> concentration from the observations (2006–2012), then dividing by the daily means to give a diurnal fraction. Diurnal changes are averaged over the whole dataset. Lines are black, red, turquoise, green and magenta for mean of observations, “no hal”, standard GEOS-Chem (v9-2), “just iodine” and iodine simulation respectively. Individual years of observational data are shown in grey.

**Iodine's impact on tropospheric oxidants: a global model study in GEOS-Chem**

T. Sherwen et al.

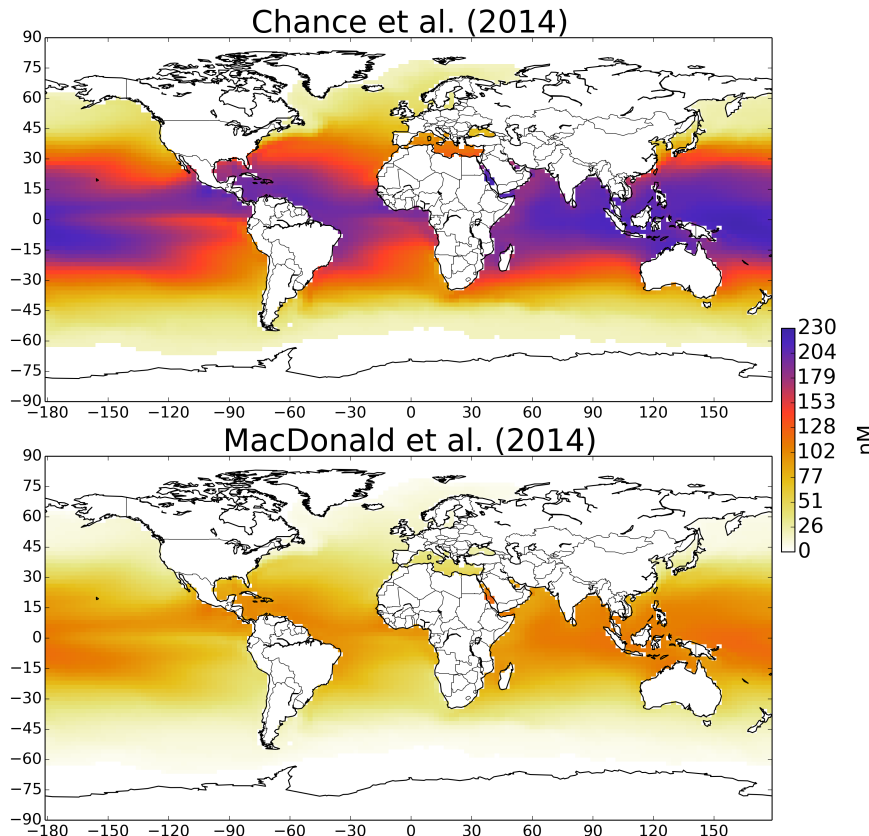


**Figure 15.** Calculated annual mean ocean surface iodide concentrations ( $\text{I}^-$ ) in nM. Values are calculated from the highest correlation relationship (square) presented in Chance et al. (2014) Table 2 (top) and from Arrhenius relationship from Eq. (1) in MacDonald et al. (2014) (bottom). The Chance et al. (2014) parameterisation is used as the standard in the work with the MacDonald et al. (2014) used as the “Ocean iodide” sensitivity simulation in Sect. 7.

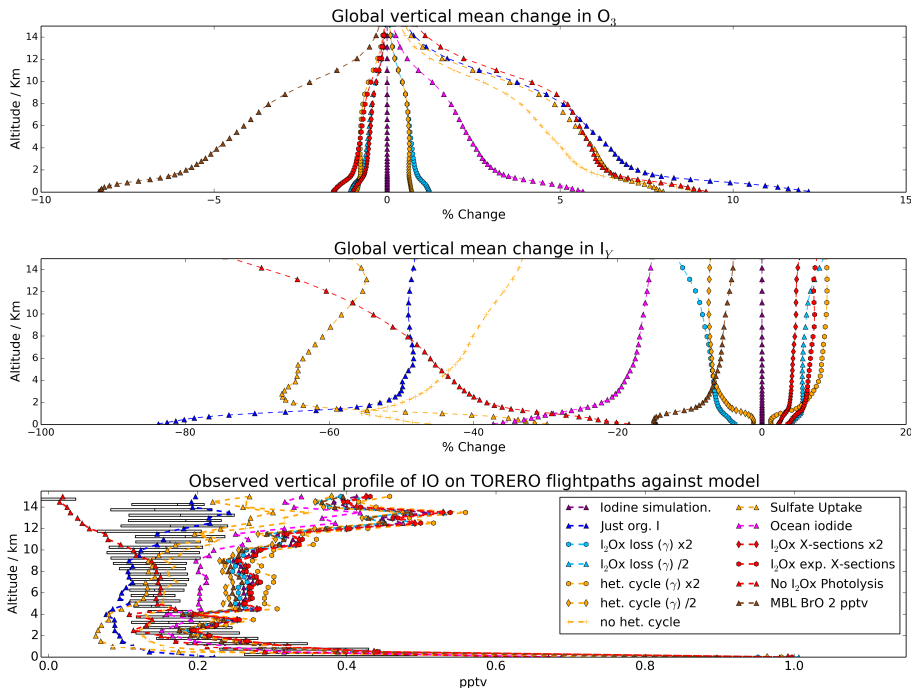


**Figure 16.** Sensitivity impacts. Upper and middle panels show global mean vertical percentage changes in concentrations of  $O_3$ , and  $I_Y$ . Lower panel gives vertically averaged iodine oxide (IO) mixing ratios (pptv) calculated along the TORERO Volkamer et al. (2015); Wang et al. (2015) flightpaths. The legend (bottom) is shared by all plots. The boxplot of IO observations (black) represents the quartiles of the data, with the median shown within the box.